

HPPP: Halpern-type Preconditioned Proximal Point Algorithms and Applications to Image Restoration

Shuchang Zhang*, Hui Zhang[†], and Hongxia Wang[‡]

Abstract. Preconditioned Proximal Point (PPP) algorithms provide a unified framework for splitting methods in image restoration. Recent advancements with RED (Regularization by Denoising) and PnP (Plug-and-Play) priors have achieved state-of-the-art performance in this domain, emphasizing the need for a meaningful particular solution. However, degenerate PPP algorithms typically exhibit weak convergence in infinite-dimensional Hilbert space, leading to uncertain solutions. To address this issue, we propose the Halpern-type Preconditioned Proximal Point (HPPP) algorithm, which leverages the strong convergence properties of Halpern iteration to achieve a particular solution. Based on the implicit regularization defined by gradient RED, we further introduce the **Gradient REgularization by Denoising via HPPP** called **GraRED-HP³** algorithm. The HPPP algorithm is shown to have the regularity converging to a particular solution by a toy example. Additionally, experiments in image deblurring and inpainting validate the effectiveness of GraRED-HP³, showing it surpasses classical methods such as Chambolle-Pock (CP), PPP, RED, and RED-PRO.

Key words. Halpern iteration, Preconditioned proximal point algorithms, RED, Image restoration

1. Introduction. Image restoration (IR) problems, including image deblurring, super-resolution, and inpainting, can be formulated as the following optimization problem [10, 20]:

$$(1.1) \quad \min_{\mathbf{x} \in \mathcal{X}} \lambda f(\mathbf{x}) + g(\mathbf{K}\mathbf{x}),$$

where $f : \mathcal{X} \rightarrow \mathbb{R} \cup \{+\infty\}$ and $g : \mathcal{Y} \rightarrow \mathbb{R} \cup \{+\infty\}$ are convex, lower semicontinuous functions, $\mathbf{K} : \mathcal{X} \rightarrow \mathcal{Y}$ is a bounded linear operator, and $\lambda > 0$ is a balance parameter. Both \mathcal{X} and \mathcal{Y} are real Hilbert spaces. The first term f represents the data fidelity, while the second term g serves as a regularization (or prior) to mitigate the ill-posedness of IR problems. Examples include total variation (TV) regularization $\|\nabla \mathbf{x}\|_1$ ($\mathbf{K} = \nabla$) as in [34], and sparsity regularization $\|\mathbf{x}\|_1$ ($\mathbf{K} = I$).

By the first-order optimality condition, the convex optimization problem (1.1) is equivalent to the following inclusion problem:

$$(1.2) \quad \text{find } \mathbf{x} \in \mathcal{X} \text{ such that } 0 \in \lambda \partial f(\mathbf{x}) + \mathbf{K}^* \partial g(\mathbf{K}\mathbf{x}),$$

where $\partial f(\mathbf{x})$ and $\partial g(\mathbf{x})$ are the subdifferentials of f and g at \mathbf{x} , respectively [4, Chapter 3]. Following [20, 5], by introducing an auxiliary variable $\mathbf{y} \in \partial g(\mathbf{K}\mathbf{x})$, we can reformulate (1.2) as:

$$(1.3) \quad \text{find } \mathbf{u} \in \mathcal{H} \text{ such that } \mathbf{0} \in \mathcal{A}\mathbf{u},$$

where $\mathcal{A} = \begin{pmatrix} \lambda \partial f & \mathbf{K}^* \\ -\mathbf{K} & (\partial g)^{-1} \end{pmatrix}$, $\mathbf{u} = (\mathbf{x}, \mathbf{y})$, and $\mathcal{H} = \mathcal{X} \times \mathcal{Y}$. The problem (1.3) is common in modern optimization and variational analysis [1, 2]. When \mathcal{A} is maximal monotone, the

*Department of Mathematics, National University of Defense Technology (zhangshuchang19@nudt.edu.cn).

[†]Department of Mathematics, National University of Defense Technology (h.zhang1984@163.com).

[‡]Corresponding author. National University of Defense Technology (wanghongxia@nudt.edu.cn).

resolvent $J_{\mathcal{A}} = (I + \mathcal{A})^{-1}$ is nonexpansive with a full domain, as established by the Minty surjectivity theorem [27]. The proximal point iteration $\mathbf{u}^{k+1} = (I + \mathcal{A})^{-1}\mathbf{u}^k$ is used to solve (1.3) and has been proven to converge weakly [32]. Since the resolvent $(I + \mathcal{A})^{-1}$ is generally difficult to compute, splitting methods have been proposed to address this issue. The well-known Douglas-Rachford splitting (DRS) [16] decomposes \mathcal{A} into the sum of two maximal monotone operators \mathcal{A}_1 and \mathcal{A}_2 , for which the resolvents $J_{\mathcal{A}_1}$ and $J_{\mathcal{A}_2}$ are easier to obtain. Another popular splitting algorithm is the Chambolle-Pock (CP) algorithm [10, 30], which solves the saddle-point problem of (1.1), i.e.,

$$(1.4) \quad \min_{\mathbf{x} \in \mathcal{X}} \max_{\mathbf{y} \in \mathcal{Y}} \langle \mathbf{K}\mathbf{x}, \mathbf{y} \rangle + \lambda f(\mathbf{x}) - g^*(\mathbf{y}),$$

where $g^* : \mathcal{K} \rightarrow \mathbb{R}^+$ is the Fenchel conjugate functional. He and Yuan [21] were the first to analyze the Primal-Dual Hybrid Gradient (PDHG) by the preconditioned proximal point (PPP) method, given by $\mathbf{0} \in \mathcal{A}\mathbf{u}^{k+1} + \mathcal{M}(\mathbf{u}^{k+1} - \mathbf{u}^k)$ with a positive definite preconditioner $\mathcal{M} : \mathcal{H} \rightarrow \mathcal{H}$. Bredies et al. [6, 7, 5] developed a unified degenerate PPP algorithmic framework with a semi-definite preconditioner. Assuming that $\mathcal{T} = (\mathcal{A} + \mathcal{M})^{-1}\mathcal{M}$ has a full domain and is single-valued, the PPP method with the classic Krasnosel'skii-Mann (KM) iteration solves for the fixed point of \mathcal{T} , i.e., $\mathcal{T}(\mathbf{u}) = \mathbf{u}$. From the perspective of degenerate PPP [5], both DRS and CP splitting algorithms can be considered as special cases of the PPP algorithm with proper preconditioner.

However, PPP algorithms with a semi-definite preconditioner generally exhibit weak convergence in Hilbert space, resulting in uncertain solutions. It is meaningful to study the limit point of sequences generated by PPP, Bauschke et al. obtained strong convergence results of PPP in the special case of linear relation on \mathcal{A} [2], the fixed-point set $\text{Fix}(\mathcal{T})$ is a linear subspace, the weak limit of the PPP sequence is the \mathcal{M} -projection of initial point. The classic Halpern iteration [19] offers the advantage of strong convergence over other iterations (such as the KM iteration) in infinite-dimensional Hilbert spaces, with the limit identified as the metric projection of the anchor onto the fixed point set [22]. This method is also known as an implicit regularization technique [15, 31]. Due to this implicit bias (projection onto solutions), degenerate PPP algorithms incorporating Halpern iteration are more likely to approximate the true solution, yielding better recovery results for IR problems. Besides the benefit of converging to a particular fixed point, Halpern iteration also possesses acceleration properties widely utilized in machine learning [15, 29]. Even without theoretical guarantees, literature [29] has demonstrated that PDHG with Halpern iteration achieves a faster convergence rate for function values in CT image reconstruction.

Recently, first-order optimization algorithms (steepest decent (SD), fixed-point (FP) iteration and ADMM) have played an critical role in implicit regularization, such as PnP priors [38] and RED [33], which have achieved state-of-the-art performance in IR problems [8, 43, 25, 37]. PnP methods by replacing proximal operators with denoisers do not seek the minimization of an explicit objective function, which strongly limits their interpretation [14, 25]. The RED prior defines a convex function whose gradient corresponds to the denoising residual itself, formulating a clear and well-defined objective function [14]. Thus, the gradient of RED can be used by these first-order optimization methods. To prove the global convergence of RED, based on fixed-point projection, Cohen et al. proposed the RED-PRO model [14] to bridge

between RED and PnP using the hybrid steepest descent method (HSD) [41]. Assuming that the data term f is a strong convexity function and the residual of the denoising neural network is nonexpansive, Ryu et al. proved the convergence of PnP-FBS(Forward-Backward Splitting) and PnP-ADMM by the classical Banach contraction principle [35], but imposing strong convexity on f excludes many IR tasks [25]. To overcome the strong convexity assumption, Hurault et al. proposed proximal denoisers of PnP methods, and the gradient step denoiser [13, 24] can be interpreted as a proximal operator of implicit regularization [25]. However, these works did not obtain the particular solution. It is crucial to obtain a unique, stable, and particular solution for IR problems [17].

Since the Halpern iteration can naturally obtain the particular solution (initial point projection onto the fixed-point set). Therefore, Halpern-type preconditioned proximal point called HPPP (1.5) is proposed to tackle the above issue, i.e.,

$$(1.5) \quad \mathbf{u}^{k+1} = \mu_{k+1} \mathbf{a} + (1 - \mu_{k+1}) \mathcal{T}(\mathbf{u}^k),$$

where $\mathbf{a}, \mathbf{u}^0 \in \mathcal{H}$ are the anchor point and the initial point, respectively, $\mathcal{T} = (\mathcal{M} + \mathcal{A})^{-1} \mathcal{M}$ is a \mathcal{M} -FNE operator (2.2) and $\{\mu_k\}$ satisfies $\sum_{k \in \mathbb{N}} \mu_k = +\infty, \mu_k \rightarrow 0 (k \rightarrow \infty)$. In addition to TV, implicit regularization such as PnP prior is also suitable for HPPP. Under the nonexpansive assumption, we find that the residual of the denoiser can also be interpreted as the proximal operator of the implicit regularization via Moreau decomposition, making it straightforward to integrate into the primal-dual algorithm with the special semi-definite preconditioner \mathcal{M} . These splitting algorithms can be viewed as fixed-point iterations from the perspective of PPP. Based on HPPP and implicit regularization,¹ we propose the implicit Gradient Regularization by Denoising via HPPP called GraRED-HP³ (see Algorithm 3.1) for IR problems. Not only can it converge to a particular solution, but it also leverages the data adaptivity of implicit regularization. This integration enriches the theoretical and algorithmic understanding of RED and PnP priors. The main contributions are as follows:

1. Theoretically, under the semi-definite preconditioner, we analyze the convergence of HPPP in Hilbert space. Compared with PPP, the proposed HPPP has the advantage of converging to a unique particular solution $\mathbf{u}^* = \arg \min_{\mathbf{u} \in \text{Fix}(\mathcal{T})} \|\mathbf{u} - \mathbf{a}\|_{\mathcal{M}}^2$ (Lemma A.3), which extends the results of the classic Halpern iteration. Let $\{\mathbf{u}^k\}_{k \in \mathbb{N}}$ be the sequence generated by HPPP; we establish an $\mathcal{O}(\frac{1}{k})$ convergence rate for $\|\mathcal{T}\mathbf{u}^k - \mathbf{u}^k\|$ and $\|\mathbf{u}^{k+1} - \mathbf{u}^k\|$.
2. Based on the special preconditioner \mathcal{M} , the primal-dual algorithm to solve (1.4) is viewed as the fixed-point iteration $\mathbf{u}^{k+1} = \mathcal{T}\mathbf{u}^k$. We apply TV or implicit regularization to HPPP, then propose the GraRED-HP³ algorithm for image restoration problems, further discuss the relationship between PnP-ADMM, GraRED-P³ (GraRED via PPP), and the proposed algorithm.
3. We numerically verify the regularity of HPPP with a simple 1D example, and further demonstrate the state-of-the-art performance of GraRED-HP³ on image deblurring and inpainting experiments. The results show that GraRED-HP³ outperforms the

¹Since the gradient of RED is exactly the residual of the denoiser, we used the GraRED notion to denote the proximal operator of the implicit regularization.

classic CP [10] and PPP [5] algorithms with TV regularization, as well as the RED [33] and RED-PRO [14] algorithms with TNRD denoiser [12].

The rest of this paper is organized as follows. In section 2, we review some useful preliminaries for convergence analysis, including the background of PPP and implicit gradient RED. In section 3, we establish the convergence and convergence rate of HPPP and apply it to TV regularization. Based on the implicit gradient RED, we propose the GraRED-HP³ algorithm for IR problems. In section 4, we verify the regularity and efficiency of the proposed algorithms with a 1D toy example. Furthermore, we validate the performance of the proposed GraRED-HP³ algorithm through image deblurring and inpainting experiments. Finally, conclusions are presented in section 5.

2. Preliminaries. In this section, we provide some preliminaries which can analyze HPPP. We examine fundamental concepts related to the degenerate PPP and RED. Let \mathcal{H} be a real Hilbert space with inner product $\langle \cdot, \cdot \rangle$ and with the corresponding induced norm $\|\cdot\|$, $\mathcal{A} : \mathcal{H} \rightarrow 2^{\mathcal{H}}$ be a (maybe multivalued) operator.

2.1. Preconditioned proximal point. Bredies et al. [5] introduced a linear, bounded, self-adjoint and positive semi-definite operator admissible preconditioner $\mathcal{M} : \mathcal{H} \rightarrow \mathcal{H}$. The proper preconditioner \mathcal{M} can make $\mathcal{A} + \mathcal{M}$ have a lower triangular structure, which conveniently calculates $(\mathcal{A} + \mathcal{M})^{-1}\mathcal{M}$.

Definition 2.1. *An admissible preconditioner for the operator $\mathcal{A} : \mathcal{H} \rightarrow 2^{\mathcal{H}}$ is a bounded, linear, self-adjoint, and positive semi-definite operator $\mathcal{M} : \mathcal{H} \rightarrow \mathcal{H}$ such that*

$$\mathcal{T} = (\mathcal{M} + \mathcal{A})^{-1}\mathcal{M}$$

is single-valued, of full-domain, and Lipschitz continuous.

Therefore, the preconditioned proximal point iteration is written into

$$(2.1) \quad \mathbf{u}^0 \in \mathcal{H}, \mathbf{u}^{k+1} = \mathcal{T}\mathbf{u}^k = (\mathcal{M} + \mathcal{A})^{-1}\mathcal{M}\mathbf{u}^k.$$

If $\mathcal{M} = I$, then \mathcal{T} is firmly non-expansive operator [1, section 23] and (2.1) becomes the standard proximal point iteration. If \mathcal{M} is semi-definite, the property of \mathcal{T} is related with the degenerate \mathcal{M} -firmly nonexpansive (\mathcal{M} -FNE) operator [6, 9, 40, 5], which is associated with seminorm $\|\mathbf{u}\|_{\mathcal{M}} = \sqrt{\langle \mathcal{M}\mathbf{u}, \mathbf{u} \rangle}$ and semi inner-product $\langle \mathbf{u}, \mathbf{v} \rangle_{\mathcal{M}} = \langle \mathcal{M}\mathbf{u}, \mathbf{v} \rangle$.

The following notion extends monotone characteristics, i.e., \mathcal{M} -monotonicity.

Definition 2.2 (\mathcal{M} -monotonicity). *Let $\mathcal{M} : \mathcal{H} \rightarrow \mathcal{H}$ be a bounded linear positive semi-definite operator, then $\mathcal{B} : \mathcal{H} \rightarrow 2^{\mathcal{H}}$ is \mathcal{M} -monotone if we have*

$$\langle \mathbf{v} - \mathbf{v}', \mathbf{u} - \mathbf{u}' \rangle_{\mathcal{M}} \geq 0, \forall (\mathbf{u}, \mathbf{v}), (\mathbf{u}', \mathbf{v}') \in \mathcal{B}.$$

According to [5, Lemma 2.6], if $\mathcal{M}^{-1}\mathcal{A}$ is \mathcal{M} -monotone, then \mathcal{T} is \mathcal{M} -FNE, i.e.,

$$(2.2) \quad \|\mathcal{T}\mathbf{u} - \mathcal{T}\mathbf{v}\|_{\mathcal{M}}^2 + \|(I - \mathcal{T})\mathbf{u} - (I - \mathcal{T})\mathbf{v}\|_{\mathcal{M}}^2 \leq \|\mathbf{u} - \mathbf{v}\|_{\mathcal{M}}^2.$$

By the KM iteration, the relaxed PPP algorithm is written into

$$(2.3) \quad \mathbf{u}^{k+1} = (1 - \lambda_k)\mathbf{u}^k + \lambda_k\mathcal{T}\mathbf{u}^k,$$

where λ_k satisfies $\sum_k \lambda_k(2 - \lambda_k) = +\infty$.

2.2. Implicit Gradient RED. Romano et al. introduced an explicit regularizer called Regularization by Denoising (RED) [33] to construct an explicit objective function, which is defined by

$$(2.4) \quad g(\mathbf{x}) = \frac{1}{2} \langle \mathbf{x}, \mathbf{x} - D_\sigma(\mathbf{x}) \rangle,$$

where $D_\sigma : \mathbb{R}^n \rightarrow \mathbb{R}^n$ is a denoiser ($\sigma > 0$ denotes a noise level). If $D_\sigma(\mathbf{x})$ satisfies homogeneity $D_\sigma(c\mathbf{x}) = cD_\sigma(\mathbf{x}) (\forall c > 0)$ and has symmetric Jacobian, then $\nabla g(\mathbf{x}) = \mathbf{x} - D_\sigma(\mathbf{x})$. Under the following nonexpansive Assumption (A) [35] on residual $R = I - D_\sigma$, i.e.,

$$(A) \quad \|(\mathbf{x} - D_\sigma(\mathbf{x})) - (\mathbf{y} - D_\sigma(\mathbf{y}))\| \leq \|\mathbf{x} - \mathbf{y}\|, \forall \mathbf{x}, \mathbf{y} \in \mathbb{R}^n,$$

we will prove that there exists an implicit regularization ϕ such that $R(\mathbf{x}) = \nabla g(\mathbf{x}) = \text{prox}_{\phi^*}(\mathbf{x})$, where ϕ^* is the conjugate of ϕ . Here is the definition of the proximal operator and characterization of proximal operators.

Definition 2.3. [4, Section 6] Given a function $\phi : \mathbb{R}^n \rightarrow \mathbb{R}^+$, the proximal operator of $\phi(\mathbf{x})$ is defined by

$$(2.5) \quad \text{prox}_\phi(\mathbf{x}) = \arg \min_{\mathbf{u} \in \mathbb{R}^n} \frac{1}{2} \|\mathbf{u} - \mathbf{x}\|^2 + \phi(\mathbf{x}).$$

Proposition 2.4 ([28, 18]). A function $h : \mathbb{R}^n \rightarrow \mathbb{R}^n$ defined everywhere is the proximal operator of a proper convex l.s.c. (lower semicontinuous) function $\phi : \mathbb{R}^n \rightarrow \mathbb{R}^+$ if, and only if the following conditions hold jointly:

- (a) there exists a (convex l.s.c.) function ψ such that for each $\mathbf{x} \in \mathbb{R}^n$, $h(\mathbf{x}) = \nabla \psi(\mathbf{x})$;
- (b) h is nonexpansive, i.e.,

$$\|h(\mathbf{x}) - h(\mathbf{y})\| \leq \|\mathbf{x} - \mathbf{y}\|, \forall \mathbf{x}, \mathbf{y} \in \mathbb{R}^n.$$

Lemma 2.5. Assume that a denoiser $D_\sigma : \mathbb{R}^n \rightarrow \mathbb{R}^n$ satisfies homogeneity and Assumption (A), and has symmetric Jacobian, then the gradient of RED defines an implicit regularization $\phi : \mathbb{R}^n \rightarrow \mathbb{R}^+$ such that

$$(2.6) \quad R(\mathbf{x}) = \nabla g(\mathbf{x}) = \text{prox}_{\phi^*}(\mathbf{x}), D_\sigma(\mathbf{x}) = \text{prox}_\phi(\mathbf{x}).$$

Proof. Let $\psi(\mathbf{x}) = \frac{1}{2} \langle \mathbf{x}, \mathbf{x} - D_\sigma(\mathbf{x}) \rangle$, $h(\mathbf{x}) = R(\mathbf{x})$ in Proposition 2.4. By Assumption (A), there exist a function denoted ϕ^* (ϕ^* is the conjugate of ϕ) such that $R(\mathbf{x}) = \nabla g(\mathbf{x}) = \text{prox}_{\phi^*}(\mathbf{x})$. By Moreau decomposition [4, Theorem 6.44], $D_\sigma(\mathbf{x}) = \text{prox}_\phi(\mathbf{x})$. ■

3. Halpern-type preconditioned proximal point (HPPP). Compared to KM iteration, Halpern iteration [19] is an effective method to find a particular fixed point, i.e.,

$$(3.1) \quad \mathbf{u}^{k+1} = \lambda_{k+1} \mathbf{u}^0 + (1 - \lambda_{k+1}) T \mathbf{u}^k,$$

the sequence $\{\mathbf{u}^k\}_{k \in \mathbb{N}}$ with suitable $\{\lambda_k\}_{k \in \mathbb{N}}$ strongly converges to the projection of the initial point \mathbf{u}^0 to $\text{Fix}(T)$ [19, 26, 39], i.e., $\mathbf{u}^* = P_{\text{Fix}(T)}(\mathbf{u}^0)$, where $P_\Omega(\mathbf{u}^0) = \arg \min_{\mathbf{u} \in \Omega} \|\mathbf{u} - \mathbf{u}^0\|^2$ denotes the standard metric projection. Using the PPP to solve the inclusion problem (1.3),

the fixed point of \mathcal{T} is the solution of (1.3). Choosing an appropriate anchor point, such as the degraded image or an image filled with ones or zeros, can bring the projection closer to the ground-truth solution, resulting in better restoration performance. Hence, the HPPP algorithm (1.5) theoretically converges to the ground-truth solution under some known anchor point prior \mathbf{a} . When \mathcal{T} satisfies the mild condition $\|\mathcal{T}\mathbf{u} - \mathcal{T}\mathbf{v}\| \leq C\|\mathbf{u} - \mathbf{v}\|_{\mathcal{M}}$ ($C > 0$) [5], the HPPP algorithm is able to find a unique solution \mathbf{u}^* of (1.3), where $\mathbf{u}^* = \arg \min_{\mathbf{u} \in \text{Fix}(\mathcal{T})} \|\mathbf{u} - \mathbf{a}\|_{\mathcal{M}}^2$ (see Lemma A.3).

3.1. Convergence analysis. Firstly, we analyze the convergence of HPPP, the sequence $\{\mathbf{u}^k\}$ generated by HPPP (1.5) converges to a particular fixed point. The strong and weak convergences are denoted \rightarrow and \rightharpoonup , respectively.

Theorem 3.1. *Let $\mathcal{A} : \mathcal{H} \rightarrow 2^{\mathcal{H}}$ be an operator with $\text{zer}\mathcal{A} \neq \emptyset$, and \mathcal{M} an admissible preconditioner such that $(\mathcal{M} + \mathcal{A})^{-1}$ is L -Lipshitz. Let $\{\mathbf{u}^k\}$ be the sequence generated by HPPP (1.5). Assume that every weak cluster point of $\{\mathbf{u}^k\}_{k \in \mathbb{N}}$ lies in $\text{Fix}(\mathcal{T})$, and $\{\mu_k\}_{k \in \mathbb{N}}$ satisfies*

- (i) $\lim_{k \rightarrow \infty} \mu_k = 0$;
- (ii) $\sum_{k \in \mathbb{N}} \mu_k = +\infty$;
- (iii) $\lim_{k \rightarrow \infty} \frac{\mu_{k+1} - \mu_k}{\mu_k} = 0$ or $\sum_{k \in \mathbb{N}} |\mu_{k+1} - \mu_k| < \infty$.

Then \mathbf{u}^k converges strongly to \mathbf{u}^* which is the unique solution of $\min_{\mathbf{u} \in \text{Fix}(\mathcal{T})} \|\mathbf{u} - \mathbf{a}\|_{\mathcal{M}}^2$.

Proof. Firstly, we show that $\|\mathbf{u}^k - \mathbf{u}^*\|_{\mathcal{M}} \rightarrow 0$, where

$$\mathbf{u}^* = P_{\text{Fix}(\mathcal{T})}^{\mathcal{M}}(\mathbf{a}) = \arg \min_{\mathbf{u} \in \text{Fix}(\mathcal{T})} \|\mathbf{u} - \mathbf{a}\|_{\mathcal{M}}^2.$$

Then, we have

$$\begin{aligned} \|\mathbf{u}^{k+1} - \mathbf{u}^*\|_{\mathcal{M}}^2 &= \left\| \mu_{k+1}(\mathbf{a} - \mathbf{u}^*) + (1 - \mu_{k+1})(\mathcal{T}\mathbf{u}^k - \mathbf{u}^*) \right\|_{\mathcal{M}}^2 \\ &= \mu_{k+1}^2 \|\mathbf{a} - \mathbf{u}^*\|_{\mathcal{M}}^2 + (1 - \mu_{k+1})^2 \|\mathcal{T}\mathbf{u}^k - \mathbf{u}^*\|_{\mathcal{M}}^2 \\ &\quad + 2\mu_{k+1}(1 - \mu_{k+1}) \left\langle \mathbf{a} - \mathbf{u}^*, \mathcal{T}\mathbf{u}^k - \mathbf{u}^* \right\rangle_{\mathcal{M}} \\ &\leq (1 - \mu_{k+1}) \|\mathbf{u}^k - \mathbf{u}^*\|_{\mathcal{M}}^2 + \mu_{k+1} \delta_{k+1}, \end{aligned}$$

where $\delta_k = \mu_k \|\mathbf{a} - \mathbf{u}^*\|_{\mathcal{M}}^2 + 2\mu_k(1 - \mu_k) \left\langle \mathbf{a} - \mathbf{u}^*, \mathcal{T}\mathbf{u}^{k-1} - \mathbf{u}^* \right\rangle_{\mathcal{M}}$. By Lemma A.2, $\{\mathbf{u}^k\}$ is bounded, there exists $\tilde{\mathbf{u}}$ such that $\mathbf{u}^k \rightharpoonup \tilde{\mathbf{u}} \in \text{Fix}(\mathcal{T})$ according to the known condition. Assume that $\mathbf{u}^{k_n} \rightharpoonup \tilde{\mathbf{u}}$ such that

$$\begin{aligned} \limsup_{k \rightarrow \infty} \left\langle \mathbf{a} - \mathbf{u}^*, \mathbf{u}^k - \mathbf{u}^* \right\rangle_{\mathcal{M}} &= \lim_{n \rightarrow \infty} \left\langle \mathbf{a} - \mathbf{u}^*, \mathbf{u}^{k_n} - \mathbf{u}^* \right\rangle_{\mathcal{M}} \\ &= \left\langle \mathbf{a} - \mathbf{u}^*, \tilde{\mathbf{u}} - \mathbf{u}^* \right\rangle_{\mathcal{M}}. \end{aligned}$$

Since \mathbf{u}^* is the unique solution of $\min_{\mathbf{u} \in \text{Fix}(\mathcal{T})} \|\mathbf{a} - \mathbf{u}\|_{\mathcal{M}}^2$ according to Lemma A.3, which solves

$$\left\langle \mathbf{u}^* - \mathbf{a}, \mathbf{u} - \mathbf{u}^* \right\rangle_{\mathcal{M}} \leq 0, \forall \mathbf{u} \in \text{Fix}(\mathcal{T}).$$

Therefore $\limsup_{k \rightarrow \infty} \delta_k \leq 0$, from Lemma A.1 we obtain $\lim_{k \rightarrow \infty} \|\mathbf{u}^k - \mathbf{u}^*\|_{\mathcal{M}} = 0$. we then prove $\|\mathbf{u}^k - \mathbf{u}^*\| \rightarrow 0$.

$$\begin{aligned} \|\mathbf{u}^{k+1} - \mathbf{u}^*\| &= \left\| \mu_{k+1}(\mathbf{a} - \mathbf{u}^*) + (1 - \mu_{k+1})(\mathcal{T}\mathbf{u}^k - \mathbf{u}^*) \right\| \\ &\leq \mu_{k+1} \|\mathbf{a} - \mathbf{u}^*\| + (1 - \mu_{k+1}) \|\mathcal{T}\mathbf{u}^k - \mathbf{u}^*\| \\ &\leq \mu_{k+1} \|\mathbf{a} - \mathbf{u}^*\| + C(1 - \mu_{k+1}) \|\mathbf{u}^k - \mathbf{u}^*\|_{\mathcal{M}}, \end{aligned}$$

it easily follows that $\|\mathbf{u}^k - \mathbf{u}^*\| \rightarrow 0$ from $\mu_{k+1} \rightarrow 0$ and $\|\mathbf{u}^k - \mathbf{u}^*\|_{\mathcal{M}} \rightarrow 0$. \blacksquare

It is easy to verify that $\mu_k = \frac{1}{k^\alpha}$ ($0 < \alpha \leq 1$) satisfy conditions (i)-(iii). Under mild conditions(i)-(iii), compared with [2], we have provided an alternative method to obtain the limit point as \mathcal{M} -projection of the initial point.

Corollary 3.2. *Let $\mathcal{A} : \mathcal{H} \rightarrow 2^{\mathcal{H}}$ be a maximal operator with $\text{zer}\mathcal{A} \neq \emptyset$, and \mathcal{M} an admissible preconditioner such that $(\mathcal{M} + \mathcal{A})^{-1}$ is L -Lipshitz. Let $\{\mathbf{u}^k\}$ be the sequence generated by HPPP (1.5). If $\{\mu_k\}_{k \in \mathbb{N}}$ satisfies $\sum_{k \in \mathbb{N}} \mu_k = \infty, \mu_k \rightarrow 0 (k \rightarrow \infty), \lim_{k \rightarrow \infty} \frac{\mu_{k+1} - \mu_k}{\mu_k} = 0$ or $\sum_{k \in \mathbb{N}} |\mu_{k+1} - \mu_k| < \infty$, then \mathbf{u}^k converges strongly to \mathbf{u}^* , which is the unique solution of $\min_{\mathbf{u} \in \text{Fix}(\mathcal{T})} \|\mathbf{u} - \mathbf{a}\|_{\mathcal{M}}^2$.*

Proof. Assume that $\mathbf{u}^k \rightharpoonup \mathbf{u}, \mathcal{T}\mathbf{u}^k - \mathbf{u}^k \rightarrow 0$ (Lemma A.2), it follows that

$$\mathcal{T}\mathbf{u}^k = \mathcal{T}\mathbf{u}^k - \mathbf{u}^k + \mathbf{u}^k \rightharpoonup 0 + \mathbf{u} = \mathbf{u},$$

i.e., $\mathcal{T}\mathbf{u}^k \rightharpoonup \mathbf{u}$. From $\mathcal{T}\mathbf{u}^k - \mathbf{u}^k \rightarrow 0$ and $\mathcal{T}\mathbf{u}^k = (\mathcal{M} + \mathcal{A})^{-1} \mathcal{M}\mathbf{u}^k$ we have

$$(3.2) \quad \mathcal{A}\mathcal{T}\mathbf{u}^k \ni \mathcal{M}(\mathbf{u}^k - \mathcal{T}\mathbf{u}^k) \rightarrow 0.$$

By the maximality of \mathcal{A} we have that \mathcal{A} is closed in $\mathcal{H}_{\text{weak}} \times \mathcal{H}_{\text{strong}}$ (see [1, Proposition 20.38]), hence $0 \in \mathcal{A}\mathbf{u}$, i.e., \mathbf{u} is a fixed point of \mathcal{T} . Thus, every weak cluster point of $\{\mathbf{u}^k\}_{k \in \mathbb{N}}$ lies in $\text{Fix}(\mathcal{T})$, it holds by Theorem 3.1. \blacksquare

Remark 1. *Compared Theorem 3.1, Corollary 3.2 with [5, Theorem 2.9, convergence] and [5, Corollary 2.10], $\{\mathbf{u}^k\}_{k \in \mathbb{N}}$ generated by HPPP converges strongly to a particular fixed point of \mathcal{T} . All conditions are the same except we only add the mild assumption about $\{\mu_k\}_{k \in \mathbb{N}}$ used for convergence analysis. $\{\mathbf{u}^k\}_{k \in \mathbb{N}}, \{\mathcal{T}\mathbf{u}^k\}_{k \in \mathbb{N}}$ can converges weakly to the same fixed point of \mathcal{T} since $\|\mathcal{T}\mathbf{u}^k - \mathbf{u}^k\| \rightarrow 0$. The Lipschitz regularity of $(\mathcal{M} + \mathcal{A})^{-1}$ is a mild assumption especially in applications to splitting algorithms, which is used to prove the uniqueness of \mathcal{M} -projection and guarantee the boundedness of $\{\mathbf{u}^k\}_{k \in \mathbb{N}}, \{\mathcal{T}\mathbf{u}^k\}_{k \in \mathbb{N}}$.*

3.2. Convergence rate. In this section, we will give the result of the sub-linear convergence rate of the gap between two successive iterations. We now present a technical Lemma [36] for convergence rate.

Lemma 3.3 ([36]). *Let $M > 0$. Assume that $\{a_k\}_{k \in \mathbb{N}}$ is a sequence of nonnegative real numbers which satisfy $a_1 < M$ and*

$$a_{k+1} \leq (1 - \gamma b_{k+1})a_k + (b_k - b_{k+1})c_k, k \geq 1,$$

where $\gamma \in (0, 1]$, $\{b_k\}_{k \in \mathbb{N}}$ is a sequence which is defined by $b_k = \min\{\frac{2}{\gamma k}, 1\}$, $\{a_k\}_{k \in \mathbb{N}}$ is a sequence of real numbers such that $c_k \leq M < \infty$. Then, the sequence $\{a_k\}_{k \in \mathbb{N}}$ satisfies

$$a_k \leq \frac{MJ}{\gamma k}, k \geq 1,$$

where $J = \lfloor \frac{2}{\gamma} \rfloor$.

Corollary 3.4. Let $\mathcal{T} = (\mathcal{M} + \mathcal{A})^{-1}\mathcal{M}$ be a \mathcal{M} -FNE operator, $(\mathcal{M} + \mathcal{A})^{-1}$ is L -Lipshitz, and $\{u^k\}$ be the sequence generated by (1.5). If $\mu_k = \min\{\frac{2}{k}, 1\}$, then

- (i) $\|\mathbf{u}^{k+1} - \mathbf{u}^k\|_{\mathcal{M}} \leq \frac{2M'}{k}$, i.e., $\|\mathbf{u}^{k+1} - \mathbf{u}^k\|_{\mathcal{M}} = \mathcal{O}(\frac{1}{k})$;
- (ii) $\|\mathbf{u}^{k+1} - \mathbf{u}^k\| = \mathcal{O}(\frac{1}{k})$, $\|\mathbf{u}^k - \mathcal{T}\mathbf{u}^k\| = \mathcal{O}(\frac{1}{k})$.

Proof. For (i), denote $M' = \sup_{k \in \mathbb{N}}\{\|\mathbf{u}^0 - \mathcal{T}\mathbf{u}^k\|_{\mathcal{M}}\}$, since

$$\|\mathbf{u}^{k+1} - \mathbf{u}^k\|_{\mathcal{M}} \leq (1 - \mu_{k+1})\|\mathbf{u}^k - \mathbf{u}^{k-1}\|_{\mathcal{M}} + |\mu_{k+1} - \mu_k| M',$$

it derives (i) by Lemma 3.3. For (ii), since

$$\begin{aligned} \|\mathbf{u}^{k+1} - \mathbf{u}^k\| &\leq C(1 - \mu_{k+1})\|\mathbf{u}^k - \mathbf{u}^{k-1}\|_{\mathcal{M}} + M'|\mu_{k+1} - \mu_k| \\ &\leq \frac{2M'C}{k-1} + \frac{2M'}{k(k+1)}, k \geq 2. \end{aligned}$$

and thus $\|\mathbf{u}^k - \mathcal{T}\mathbf{u}^k\| \leq \|\mathbf{u}^k - \mathbf{u}^{k+1}\| + \mu_{k+1}\|\mathbf{a} - \mathcal{T}\mathbf{u}^k\| = \mathcal{O}(\frac{1}{k})$. ■

3.3. HPPP with TV regularization. Chambolle-Pock(CP) is a first-order primal-dual algorithm to solve non-smooth convex optimization problems with known saddle-point structure [10]. Take the starting point $(\mathbf{x}_0, \mathbf{y}_0) \in \mathcal{X} \times \mathcal{Y}$, the CP primal-dual algorithm is written into the following form:

$$(3.3) \quad \begin{cases} \mathbf{x}_{k+1} &= (I + \tau \partial f)^{-1}(\mathbf{x}_k - \tau \mathbf{K}^* \mathbf{y}_k), \\ \mathbf{y}_{k+1} &= (I + s \partial g^*)^{-1}(\mathbf{y}_k + s \mathbf{K}(2\mathbf{x}_{k+1} - \mathbf{x}_k)), \end{cases}$$

here we consider TV regularization $\mathbf{K} = \nabla$. The convergence of CP algorithm was proved when step sizes satisfy $\tau s \|\mathbf{K}\|^2 < 1$. By introducing the operator \mathcal{A} and preconditioner \mathcal{M} , set

$$(3.4) \quad \mathcal{A} = \begin{pmatrix} \partial f & \mathbf{K}^* \\ -\mathbf{K} & \partial g^* \end{pmatrix}, \mathcal{M} = \begin{pmatrix} \frac{1}{\tau} I & -\mathbf{K}^* \\ -\mathbf{K} & \frac{1}{s} I \end{pmatrix}.$$

As firstly noticed in [20, 5], the CP method is a special PPP method $0 \in \mathcal{A}\mathbf{x}^{k+1} + \mathcal{M}(\mathbf{x}^{k+1} - \mathbf{x}^k)$. Bredies et al. proved the weak convergence of the CP algorithm about the degenerate case $\tau s \|\mathbf{K}\|^2 = 1$ [5], i.e., \mathcal{M} is a semi-definite preconditioner. To apply HPPP with TV regularization, under the degenerate case $\tau s \|\mathbf{K}\|^2 = 1$ we obtain

$$(3.5) \quad \begin{cases} \mathbf{x}_{k+1} &= \mu_{k+1}\mathbf{x}_a + (1 - \mu_{k+1})(I + \tau \partial f)^{-1}(\mathbf{x}_k - \tau \mathbf{K}^* \mathbf{y}_k), \\ \mathbf{y}_{k+1} &= \mu_{k+1}\mathbf{y}_a + (1 - \mu_{k+1})(I + s \partial g^*)^{-1} \left(\frac{2s\mathbf{K}(\mathbf{x}_{k+1} - \mu_{k+1}\mathbf{x}_a)}{1 - \mu_{k+1}} - s\mathbf{K}\mathbf{x}_k + \mathbf{y}_k \right), \end{cases}$$

where $\mathbf{a} = (\mathbf{x}_a, \mathbf{y}_a)$, $(\mathbf{x}_0, \mathbf{y}_0) \in \mathcal{X} \times \mathcal{Y}$ are the anchor and initial points, respectively, and μ_k satisfies conditions(i)-(iii) of Theorem 3.1.

3.4. HPPP with implicit regularization. Recently, RED frameworks have achieved state-of-the-art performance for inverse problems by utilizing CNN (convolutional neural network) denoiser as regularization [14], such as DnCNN [45]. Ryu et al. proposed a nonexpansive residual of DnCNN to ensure the convergence of PnP methods [35]. Gradient step denoisers, defined as $D_\sigma = I - \nabla g_\sigma$ for Gaussian noise level σ , have been proposed to generalize RED [13, 24], where $g_\sigma : \mathbb{R}^n \rightarrow \mathbb{R}$ is a scalar function parameterized by a differentiable neural network. The gradient step denoiser can be interpreted as the proximal operator of an implicit regularization [25].

The primal-dual algorithm to solve (1.4) is viewed as the fixed-point iteration $\mathbf{u}^{k+1} = \mathcal{T}\mathbf{u}^k = (\mathcal{A} + \mathcal{M})^{-1}\mathcal{M}\mathbf{u}^k$ with $\mathcal{A} = \begin{pmatrix} \lambda\partial f & \mathbf{K}^* \\ -\mathbf{K} & (\partial g)^{-1} \end{pmatrix}$, $\mathcal{M} = \begin{pmatrix} \frac{1}{\tau}I & -\mathbf{K}^* \\ -\mathbf{K} & \frac{1}{s}I \end{pmatrix}$ to solve (1.3). According to subsection 2.2, $R(\mathbf{x}) = \text{prox}_{\phi^*}(\mathbf{x})$, we consider the special application $g = \phi$, $\mathbf{K} = I$ with the degenerate $\mathcal{M}(\tau s = 1)$.

The proposed HPPP algorithm has the advantage of converging to a particular solution than PPP. Due to the data adaptability of CNN, which has the powerful expressiveness to represent the implicit regularization ϕ [43, 44]. Based on HPPP and GraRED, we propose the implicit Gradient RED via HPPP called GraRED-HP³ (see Algorithm 3.1). According to (2.3), we further discuss GraRED-P³ Algorithm 3.2 for IR problems.

PnP-ADMM [38, 11, 35] is a well-known optimization method to solve (1.1) when $g = \phi$, i.e.,

$$(3.6) \quad \begin{aligned} \mathbf{z}^{k+1} &= \text{prox}_\phi(\mathbf{v}^k - \bar{\mathbf{u}}^k) = D_\sigma(\mathbf{v}^k - \bar{\mathbf{u}}^k), \\ \mathbf{v}^{k+1} &= \text{prox}_{\lambda f}(\mathbf{z}^{k+1} + \bar{\mathbf{u}}^k), \\ \bar{\mathbf{u}}^{k+1} &= \bar{\mathbf{u}}^k + \mathbf{z}^{k+1} - \mathbf{v}^{k+1}. \end{aligned}$$

Let $\mathbf{w}^k = \mathbf{v}^k + \bar{\mathbf{u}}^k$, then PnP-ADMM can be written into equivalent Douglas-Rachford Splitting (DRS) form:

$$(3.7) \quad \mathbf{w}^{k+1} = \mathbf{w}^k + D_\sigma(2\text{prox}_{\lambda f}(\mathbf{w}^k) - \mathbf{w}^k) - \text{prox}_{\lambda f}(\mathbf{w}^k).$$

Using $\mathbf{w}^k = \mathbf{x}^k - \mathbf{y}^k$, $\tau = s = 1$, $\lambda_k = 1$ in GraRED-P³ results exactly in the above DRS iteration. Thus, PnP-ADMM can be obtained from the perspective of PPP [6, 5], and its convergence follows by [5, Corollary 2.15].

The following Theorem 3.5 verifies the convergence of Algorithm 3.2 and Algorithm 3.2.

Theorem 3.5. *Assume that a denoiser $D_\sigma : \mathcal{H} \rightarrow \mathcal{H}$ satisfies homogeneity and Assumption (A), and has symmetric Jacobian, relaxing parameter $0 < \inf_k \lambda_k \leq \sup_k \lambda_k < 2$ and RED is convex, then $\{\mathbf{x}^k\}_{k \in \mathbb{N}}$ generated by Algorithm 3.2 converges to some uncertain solution \mathbf{x}^* of (1.1), while $\{\mathbf{x}^k\}_{k \in \mathbb{N}}$ generated by Algorithm 3.1 converges to the particular solution $P_{\text{Fix}(\mathcal{T})}^{\mathcal{M}}(\mathbf{a})$ of (1.3).*

Proof. Followed by [5, Corollary 2.10] and Corollary 3.2. ■

Algorithm 3.1 GraRED-HP³

Input: initialization $\mathbf{u}^0 = (\mathbf{x}^0, \mathbf{y}^0) \in \mathbb{R}^n \times \mathbb{R}^n$, anchor point $\mathbf{a} = (\mathbf{x}_a, \mathbf{y}_a) \in \mathbb{R}^n \times \mathbb{R}^n$, iteration number $N > 0$, diminishing anchor coefficient $\mu_k \in [0, 1], \mu_k \rightarrow 0 (k \rightarrow \infty), \sum_{k=0}^{\infty} \mu_k = +\infty$, and $R = I - D_\sigma$ is a residual of denoiser D_σ , degenerate preconditioner $\mathcal{M} = \begin{pmatrix} \frac{1}{\tau}I & -I \\ -I & \frac{1}{s}I \end{pmatrix}, \tau s \leq 1$, where I is identity matrix.

- 1: **for** $k = 0, 1, 2, \dots, N - 1$ **do**
- 2: $\mathbf{d}^k = \text{prox}_{\lambda f}(\mathbf{x}^k - \tau \mathbf{y}^k)$
- 3: $\mathbf{x}^{k+1} = \mu_k \mathbf{x}_a + (1 - \mu_k) \mathbf{d}^k$
- 4: $\mathbf{v}^{k+1} = R(s(2\mathbf{d}^k - \mathbf{x}^k) + \mathbf{y}^k)$
- 5: $\mathbf{y}^{k+1} = \mu_{k+1} \mathbf{y}_a + (1 - \mu_{k+1}) \mathbf{v}^{k+1}$
- 6: **end for**

Output: \mathbf{x}^N .

Algorithm 3.2 GraRED-P³

Input: initialization $\mathbf{u}^0 = (\mathbf{x}^0, \mathbf{y}^0) \in \mathbb{R}^n \times \mathbb{R}^n$, iteration number $N > 0$, relaxing parameter $\lambda_k \in [0, 2], R = I - D_\sigma$ is a residual of denoiser $D_\sigma, \mathcal{A} = \begin{pmatrix} \lambda \partial f & I \\ -I & \partial \phi^* \end{pmatrix}$, degenerate preconditioner $\mathcal{M} = \begin{pmatrix} \frac{1}{\tau}I & -I \\ -I & \frac{1}{s}I \end{pmatrix}, \tau s \leq 1$, where I is identity matrix.

- 1: **for** $k = 0, 1, 2, \dots, N - 1$ **do**
- 2: $\mathbf{d}^k = \text{prox}_{\lambda f}(\mathbf{x}^k - \tau \mathbf{y}^k)$
- 3: $\mathbf{x}^{k+1} = \lambda_k \mathbf{d}^k + (1 - \lambda_k) \mathbf{x}^k$
- 4: $\mathbf{y}^{k+1} = \lambda_k R(\mathbf{y}^k + s(2\mathbf{d}^k - \mathbf{x}^k)) + (1 - \lambda_k) \mathbf{y}^k$
- 5: **end for**

Output: \mathbf{x}^N .

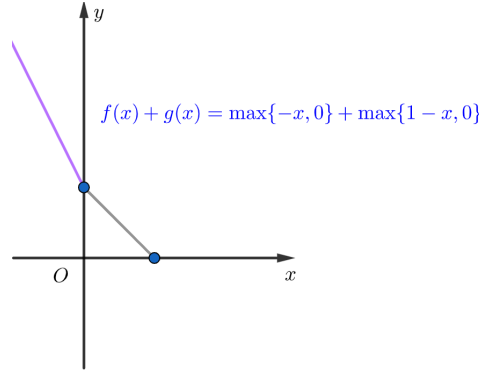
4. Experiments. In this section, we show the numerical experiments of the algorithms discussed in section 3. Firstly, we will verify the regularity of HPPP by an easy 1D example. Then, we compare the CP (3.3), PPP (2.3), GraRED-HP³ algorithms (see Algorithm 3.1), and GraRED-P³ (see Algorithm 3.2) for image deblurring and inpainting under the same setting, and verify the efficiency of the proposed algorithms.

4.1. A toy example. We consider the following optimization problem in \mathbb{R} , i.e.,

$$(4.1) \quad \min_{x \in \mathbb{R}} f(x) + g(x),$$

where $f(x) = \max\{-x, 0\}$ and $g(x) = \max\{1 - x, 0\}$ (See Figure 4.1). Since for any $y \in \mathbb{R}$,

$$\min\{(1 + y)x - 1, yx\} = \begin{cases} (1 + y)x - 1, & x < 1 \\ yx, & x \geq 1 \end{cases},$$

Figure 4.1: Plot $f(x) + g(x)$.

then $g^*(y) = \max_x [yx - \max\{1-x, 0\}] = y + \delta_{[-1,0]}(y)$, $y \in \mathbb{R}$, where

$$\delta_C(y) = \begin{cases} 0, & y \in C, \\ \infty, & y \notin C. \end{cases}$$

Therefore, the corresponding saddle-point problem is:

$$\min_{x \in \mathbb{R}} \max_{y \in \mathbb{R}} xy + f(x) - g^*(y).$$

We denote the optimal set $X^* = [1, +\infty) = \arg \min_{x \in \mathbb{R}} f(x) + g(x)$ and the primal-dual objective function $F(x, y) = xy + f(x) - g^*(y)$. Let us solve the saddle-point set $\{(x^*, y^*) : F(x^*, y) \leq F(x^*, y^*) \leq F(x, y^*), \forall (x, y) \in \mathbb{R}^2\}$ of $F(x, y)$. Fixed $x^* \geq 1$, then

$$\max_{-1 \leq y \leq 0} \{x^*y - g^*(y)\} = \max_{-1 \leq y \leq 0} \{x^*y - y\} = \begin{cases} 0, & x^* > 1, y = 0; \\ 0, & x^* = 1, y \in [-1, 0]. \end{cases}$$

If $x^* = 1$, assume that $-1 \leq y^* < 0$, then $F(1, y^*) = 0$, while $F(x, y^*) = y^*(x-1) + \max\{-x, 0\}$ and there exists $x = 2$ such that $F(2, y^*) = y^* < F(1, y^*)$, which leads to contradiction. Therefore, the saddle-point set is $\Omega = \{(x^*, y^*) : x^* \geq 1, y^* = 0\}$.

For this toy example shown in Figure 4.2, we choose the same initial point $\mathbf{u}^0 = (-6, 6)$ or $(0, 0)$, three different anchor points $\mathbf{a} = (12, 10), (12, 9), (12, 8)$, the semi-definite $\mathcal{M} = \begin{pmatrix} 1 & -1 \\ -1 & 1 \end{pmatrix}$, and the total iteration number $N = 1000$. As shown in Figure 4.2, \mathbf{u}^k generated by HPPP (1.5) can converge to the particular saddle point controlled by the anchor point. While the limit of \mathbf{u}^k generated by PPP (2.3) may be uncertain, which is related with \mathbf{u}^0 and λ_k . For example, the sequence \mathbf{u}^k oscillates around the limit $(1.8, 0)$ shown in Figure 4.2d.

As shown in Figure 4.3, $\min_{\mathbf{u} \in \text{Fix}(\mathcal{T})} \|\mathbf{u} - \mathbf{a}\|_{\mathcal{M}}^2 = \min_{(x,y) \in \Omega} (x - x_a - (y - y_a))^2$ can be geometrically interpreted as \mathcal{M} -projection, i.e., the point $\mathbf{u} \in \text{Fix}(\mathcal{T})$ projection onto the line $x - y = x_a - y_a$ through the anchor point $\mathbf{a} = (x_a, y_a)$. Therefore, the \mathcal{M} -projection of $\mathbf{a} = (x_a, y_a)$ onto Ω is definitely solved by

$$P_{\Omega}^{\mathcal{M}}(\mathbf{a}) = \begin{cases} (1, 0), & x_a - y_a - 1 \leq 0; \\ (x_a - y_a, 0), & x_a - y_a - 1 > 0. \end{cases}$$

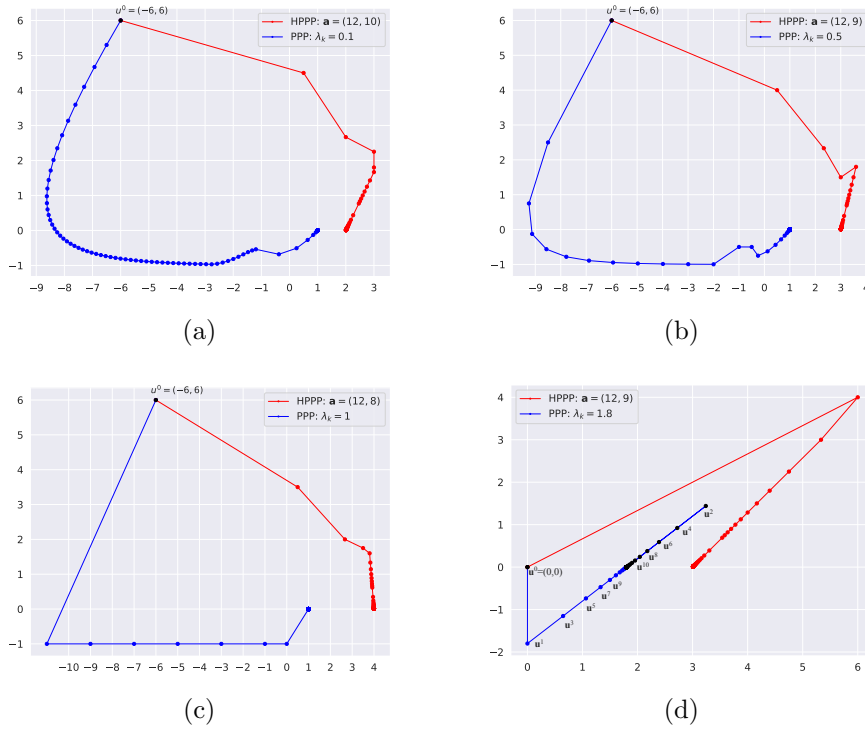


Figure 4.2: Trajectory of $\mathbf{u}^k = (x^k, y^k)$ in the xOy Cartesian coordinate system.

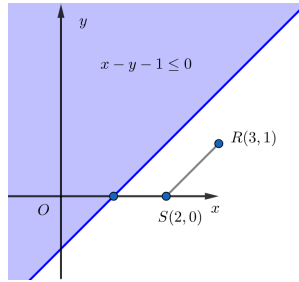


Figure 4.3: \mathcal{M} -projection onto the saddle point set.

4.2. Image deblurring. Firstly, we compared with classic TV regularization about CP [10], PPP [5], and HPPP (see details in 3.3). For classic TV $-\ell^2$ regularization,

$$(4.2) \quad \min_{\mathbf{x} \in \mathbb{R}^n} \frac{\lambda}{2} \|\mathbf{A}\mathbf{x} - \mathbf{y}\|_2^2 + \beta \|\nabla \mathbf{x}\|_1,$$

where \mathbf{y} is the degraded image, \mathbf{A} is a linear operator. In case \mathbf{Ax} can be written as a convolution, i.e., $\mathbf{Ax} = \mathbf{k} * \mathbf{x}$, where \mathbf{k} is the blurring convolution kernel. The primal-dual model of TV $-\ell^2$ deblurring is

$$(4.3) \quad \min_{\mathbf{u} \in \mathbb{R}^n} \max_{\mathbf{p} \in \mathbb{R}^n \times \mathbb{R}^n} -\langle \mathbf{u}, \operatorname{div} \mathbf{p} \rangle + \frac{\lambda}{2} \|\mathbf{Au} - \mathbf{y}\|_2^2 - \delta_P(\mathbf{p}),$$

where $f(\mathbf{u}) = \frac{\lambda}{2} \|\mathbf{Au} - \mathbf{y}\|_2^2$, $g^*(\mathbf{p}) = \delta_P(\mathbf{p})$, $P = \{\mathbf{p} \in \mathbb{R}^n \times \mathbb{R}^n : \|\mathbf{p}\|_\infty \leq \beta\}$, $\|\mathbf{p}\|_\infty$ is the discrete maximum norm defined as:

$$\|\mathbf{p}\|_\infty = \max_{i,j} |\mathbf{p}_{i,j}|, |\mathbf{p}_{i,j}| = \sqrt{(\mathbf{p}_{i,j}^1)^2 + (\mathbf{p}_{i,j}^2)^2}.$$

We can calculate the proximal operator $(I + \tau \partial g^*)^{-1}$ of the indicator $g^*(\mathbf{p})$, i.e.,

$$\mathbf{p} = (I + \tau \partial g^*)^{-1}(\tilde{\mathbf{p}}) \iff \mathbf{p}_{i,j} = \frac{\tilde{\mathbf{p}}_{i,j}}{\max(\beta, |\tilde{\mathbf{p}}_{i,j}|)}.$$

The resolvent operator for $f(\mathbf{x})$ can be computed by FFT.

$$\begin{aligned} \mathbf{x} &= (I + \tau \partial f)^{-1}(\tilde{\mathbf{x}}) \\ &= \arg \min_{\mathbf{x}} \frac{\|\mathbf{x} - \tilde{\mathbf{x}}\|}{2\tau} + \frac{\lambda}{2} \|\mathbf{k} * \mathbf{x} - \mathbf{y}\|_2^2 \\ &= \mathcal{F}^{-1} \left(\frac{\tau \lambda \mathcal{F}(\mathbf{y}) \mathcal{F}^*(\mathbf{k}) + \mathcal{F}(\tilde{\mathbf{x}})}{\tau \lambda \mathcal{F}(\mathbf{k})^2 + 1} \right), \end{aligned}$$

where $\mathcal{F}(\cdot)$ and $\mathcal{F}^{-1}(\cdot)$ denote the FFT and inverse FFT, respectively.

We use a 2D Gaussian function with a standard deviation of 1.6 to convolve 10 test gray images, and finally obtain the degraded images with an additive WGN with noise level 0.01. Firstly, we compared three algorithms, CP, PPP, and the proposed HPPP. All the algorithms use the degraded images as initial points. We calculate the norm $\|K\| = 1.75$, and choose the total iteration $N = 400$, balance coefficients $\lambda = 2$, $\beta = 5 \times 10^{-4}$. Their parameters are given in Table 4.1. Both GraRED-P³ and GraRED-HP³ use DnCNN, other parameters are used below:

- GraRED-P³ : $\tau = 1, s = 1, \lambda_k = 0.2, \lambda = 20$;
- GraRED-HP³ : $\tau = 1, s = 1, \mu_k = 1/(k + 2), \lambda = 20, \mathbf{x}_a = \mathbf{y}, \mathbf{y}_a = \mathbf{0}$.

Secondly, we compared with RED and RED-PRO. The RED-PRO model uses the hybrid steepest descent method (HSD) [41, 42] to solve IR problems. Following [33, 14], a 9×9 uniform point spread function (PSF) or a 2D Gaussian function with a standard deviation of 1.6 are used to convolve test images. We finally obtained the degraded images with an additive WGN with noise level $\sigma = \sqrt{2}$. The original RGB image is converted to the YCbCr image, PnP restoration algorithms are applied to the luminance channel, and then the reconstruction image is returned to RGB space to obtain the final image. PSNR is measured on the luminance channel of the ground truth and the restored images.

Table 4.2 shows PSNR (dB) of restoration results on CP, PPP, HPPP, GraRED-P³ and GraRED-HP³. The performance of three different methods is evaluated using PSNR measure.

The best recovery results are highlighted in bold. From Table 4.2, GraRED-P³ and GraRED-HP³ are better than classic algorithms with explicit TV regularization, which demonstrates implicit regularization is more powerful to regularize inverse imaging problems. We visualize the numerical comparison between GraRED-P³, GraRED-HP³, CP, PPP, and HPPP in Figure 4.4. To further compare the robustness of the initial points between the proposed HPPP, CP, and PPP with TV regularization. As shown in Figure 4.5, we plot their respective evolutions of PSNR values for iterations for the image **House** with 10 random initial points. The HPPP algorithm converges faster (less than 200 iterations) and achieves better PSNR values than CP and PPP algorithms. Once the anchor point is chosen, the proposed algorithm is more robust than CP and PPP algorithms for image deblurring with random initializations. To verify Corollary 3.4, we show the trend of convergence rate of the gap $\|\mathbf{u}^{k+1} - \mathbf{u}^k\|$ between two successive iterations throughout the iterations with step size $\min\{\frac{2}{k}, 1\}$ ($k \geq 1$) in Figure 4.6.

Table 4.1: Parameters on CP, PPP, and HPP with TV regularization for image deblurring.

CP	$\tau = s = 1/K = 0.57$
PPP	$\tau = s = 1/K = 0.57, \lambda_k = 1.95$ or $\lambda_k = 1.2$
HPPP	$\tau = s = 1/K = 0.57, \mu_k = \frac{1}{k+2}, \mathbf{x}_a = \mathbf{A}^T \mathbf{y}, \mathbf{y}_a = 0 \cdot \nabla \mathbf{x}_a$

Table 4.2: Deblurring results of gray images compared with CP, PPP, and HPPP about the Gauss blurring kernel.

	Cameraman	House	Pepper	Starfish	Butterfly	Craft	Parrots	Barbara	Boat
CP	26.04	30.86	25.99	27.53	27.85	25.51	26.88	24.46	28.99
PPP	26.05	30.85	25.99	27.53	27.85	25.51	26.88	24.46	28.98
HPPP(TV)	26.00	31.39	26.05	27.65	27.99	25.51	26.82	24.51	29.09
GraRED-P ³	26.87	32.51	28.34	29.16	29.70	26.90	27.95	24.66	29.68
GraRED-HP ³	26.85	32.51	28.80	29.15	29.67	27.03	27.89	24.66	29.99

From the deblurring experiment Table 4.3 and Figure 4.7, GraRED-P³ and GraRED-HP³ achieve better performance than RED, RED-PRO, and RRP, which illustrates that KM or Halpern iteration used in PPP methods is effective.

4.3. Image inpainting. In this section, we use the proposed algorithm to solve TV image inpainting problems and compare their numerical results with CP [10], PPP [5], and HPPP algorithms. The discrete image inpainting model is

$$\min_{\mathbf{x} \in \mathbb{R}^n} \lambda \|\mathbf{M} \odot \mathbf{x} - \mathbf{y}\|_F^2 + \beta \|\nabla \mathbf{x}\|_1,$$

where $\|\nabla \mathbf{x}\|_1$ is the TV regularization, λ, β are balance coefficients, \odot indicates pointwise multiplication. Then the saddle-point problem is

$$\min_{\mathbf{x} \in \mathbb{R}^n} \max_{\mathbf{p} \in \mathbb{R}^n \times \mathbb{R}^n} -\langle \mathbf{x}, \text{div} \mathbf{p} \rangle + \lambda \|\mathbf{M} \odot \mathbf{x} - \mathbf{y}\|_F^2 - \delta_P(\mathbf{p}),$$

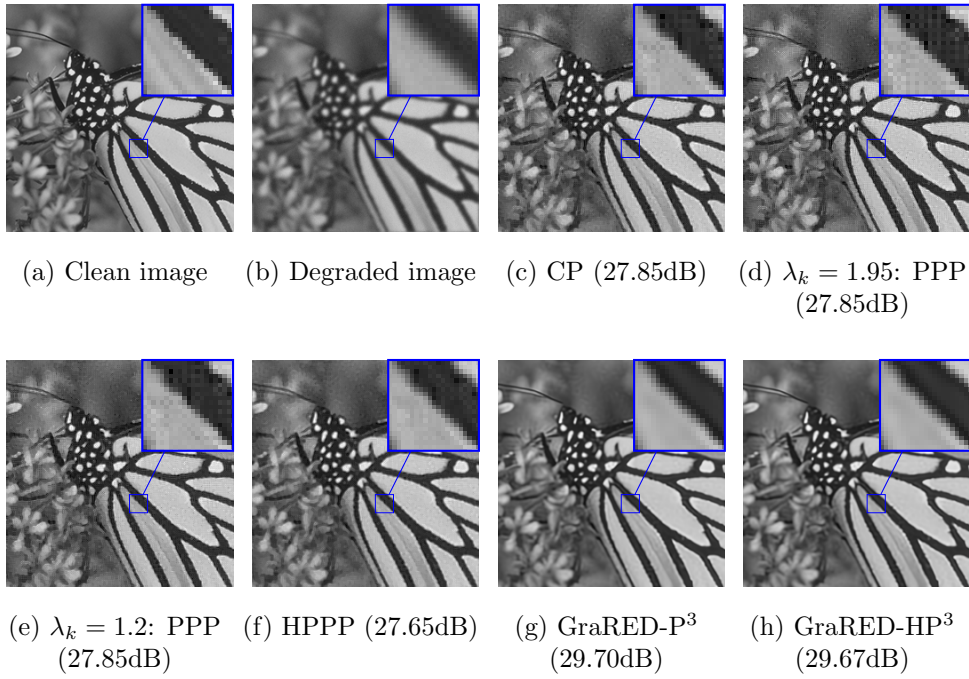


Figure 4.4: Deblurring result of **Butterfly** degraded with the Gaussian blur kernel with noise level $\sigma = 0.01$.

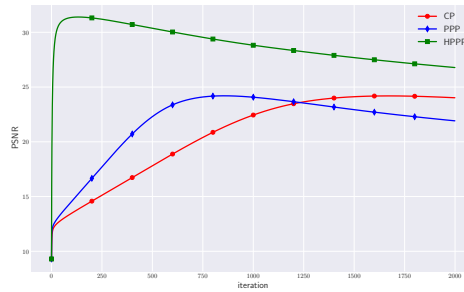


Figure 4.5: Random initialization.

where $f(\mathbf{x}) = \|\mathbf{M} \odot \mathbf{x} - \mathbf{y}\|_F^2$, $g^*(\mathbf{p}) = \delta_P(\mathbf{p})$, $P = \{\mathbf{p} \in \mathbb{R}^n \times \mathbb{R}^n : \|\mathbf{p}\|_\infty \leq \beta\}$, $\|\mathbf{p}\|_\infty$ is the discrete maximum norm. Their resolvent operators of f, g^* are

$$\mathbf{p} = (I + \tau \partial g^*)^{-1}(\tilde{\mathbf{p}}) \iff \mathbf{p}_{i,j} = \frac{\tilde{\mathbf{p}}_{i,j}}{\max(\beta, |\tilde{\mathbf{p}}_{i,j}|)}$$

and

$$\mathbf{x} = (I + \tau \partial f)^{-1}(\tilde{\mathbf{x}}) = \frac{2\tau \mathbf{M} \odot \mathbf{y} + \tilde{\mathbf{x}}}{1 + 2\tau \mathbf{M}},$$

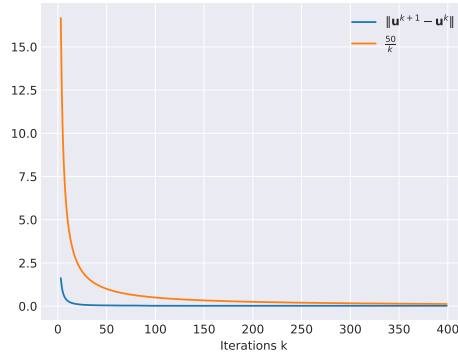


Figure 4.6: The convergence rate of $\|\mathbf{u}^{k+1} - \mathbf{u}^k\|$ of GraRED-H³. The image **Starfish** is degraded by a Gaussian PSF with noise level 0.01.

Table 4.3: Recovery results are obtained by RED, RED-PRO, RRP, GraRED-P³, and GraRED-HP³ with TNRD [12].

Algorithms	Uniform kernel				Gaussian kernel($\sigma_k = 1.6$)			
	Bike	Butterfly	Flower	Hat	Bike	Butterfly	Flower	Hat
RED [33]	26.10	30.41	30.18	32.16	27.90	31.66	32.05	33.30
RED-PRO(HSD) [14]	24.95	27.24	29.38	31.55	27.36	30.55	31.81	33.07
RRP [14]	26.48	30.64	30.46	32.25	28.02	31.66	32.08	33.26
GraRED-P ³	26.55	30.72	30.67	32.43	28.13	31.81	32.42	33.51
GraRED-HP ³	26.80	30.88	30.74	32.42	28.06	31.80	32.27	33.50

the multiplication and division operators should be understood pointwise in the above formula.

We test 10 common images for evaluation. The first \mathbf{M} is filled with a Bernoulli random mask whose each pixel is missing with probability $p = 0.5$, i.e., 50% of pixels are missed. The second \mathbf{M} is a character mask where about 19% of pixels are missed. All the algorithms start their iterations with the degraded images. For classic algorithms, we fix the balance parameter $\alpha = 0.01$ and the total number $N = 400$, and use the following other parameters :

- HPPP: $\tau = s = 1/\|K\| = 0.57$, anchor point $\mathbf{x}_a = \mathbf{1} \in \mathbb{R}^{m \times n}$, $\mathbf{y}_a = \mathbf{0} \cdot \nabla \mathbf{x}_a$, stepsize $\mu_k = \frac{1}{10(k+2)}$;
- PPP: $\tau = s = 1/\|K\| = 0.57$, $\lambda_k = 1.6$ or $\lambda_k = 1.2$;
- CP: $\tau = s = 1/\|K\| = 0.57$.

Both GraRED-P³ and GraRED-HP³ use DnCNN [35], other parameters are used below:

- GraRED-P³ : $\tau = 10$, $s = 0.1$, $\lambda_k = 0.2$, $\lambda = 5$;
- GraRED-HP³ : $\tau = 10$, $s = 0.1$, $\mu_k = 0.05/(k+2)$, $\lambda = 5$, $\mathbf{x}_a = \mathbf{y}$, $\mathbf{y}_a = \mathbf{0}$.

In Table 4.4 and Table 4.5, we compared the numerical performance of classic algorithms with TV regularization. As we can see from both two tables, the proposed two algorithms outperform other algorithms. In Figure 4.8 and 4.9, we compare visualization results of **House** degraded by Bernoulli random mask and character mask, the proposed algorithms



Figure 4.7: Deblurring result of **Butterfly** degraded by uniform kernel.

achieve better visual performance than TV regularization.

Moreover, we compare the recovery results about different anchors $\mathbf{a} = (\mathbf{x}_a, \mathbf{y}_a)$ with fixed $\mathbf{y}_a = \mathbf{0}$ and step size $\frac{1}{k+1}$. As shown in Figure 4.10, the anchor $\mathbf{x}_a = \mathbf{1}$ can achieve the best performance for random inpainting, which illustrates the projection point $P_{\text{Fix}(\mathcal{T})}^{\mathcal{M}}(\mathbf{a})$ of $\mathbf{a} = (\mathbf{1}, \mathbf{0})$ is closest to the true solution. Anchors selection is not difficult, GraRED-HP³ can achieve similar performance with other anchors.

Table 4.4: Numerical results of image inpainting compared with CP, PPP, and HPPP (noise level $\sigma = 0.01$, Bernoulli random missing).

	Cameraman	House	Peppers	Starfish	Butterfly	Craft	Parrots	Barbara	Boat
CP	23.54	28.94	24.53	23.89	23.59	23.42	23.20	23.10	26.29
PPP	23.58	29.05	24.53	24.32	23.76	23.43	23.33	23.13	26.36
HPPP(TV)	23.89	29.19	24.55	24.46	24.04	23.52	23.44	23.35	26.45
GraRED-P ³	29.92	36.15	32.67	31.99	31.95	29.53	30.05	32.25	32.91
GraRED-HP ³	29.90	36.14	32.68	31.97	31.92	29.52	30.04	32.23	32.90

5. Conclusions. In this paper, based on Halpern iteration and gradient RED, we propose HPPP and GraRED-HP³ for IR problems, which can converge strongly to a particular fixed

Table 4.5: Numerical results of image inpainting compared with CP, PPP, and HPPP (noise level $\sigma = 0.01$, character texture missing).

	Cameraman	House	Peppers	Starfish	Butterfly	Craft	Parrots	Barbara	Boat
CP	25.87	31.58	29.40	26.16	25.60	26.33	25.20	24.21	25.23
PPP	26.33	31.78	30.13	26.86	26.08	26.47	25.64	27.32	28.05
HPPP	26.33	32.00	30.02	26.88	26.38	26.51	25.83	27.34	28.09
GraRED-P ³	29.18	37.46	33.79	30.89	29.45	29.20	26.04	29.68	30.04
GraRED-HP ³	29.13	37.47	33.80	30.93	29.42	29.20	26.02	29.60	30.04

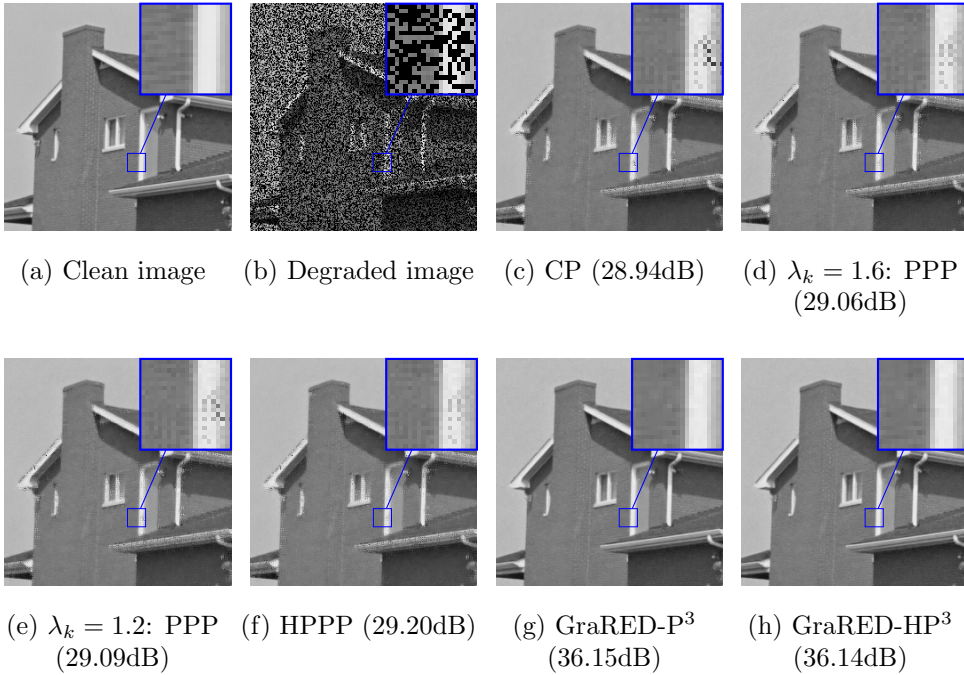


Figure 4.8: Recovery results of **House** degraded by random mask.

point $P_{\text{Fix}(\mathcal{T})}^{\mathcal{M}}$ (a). Numerical experiments verify the regularity of HPPP, and the effectiveness GraRED-HP³ for image deblurring and inpainting, which can achieve better performance than classic algorithms with TV regularization. In the future, we plan to study the convergence of nonconvex implicit regularization [25] and extend the definition of \mathcal{M} -monotonicity to \mathcal{M} -comonotonicity for nonconvex case [3].

Appendix A. Boundedness and \mathcal{M} -projection. Firstly, we study the boundedness and asymptotic regularity of $\{\mathbf{u}^k\}_{k \in \mathbb{N}}$ generated by (1.5). To further establish regularity of $\{\mathbf{u}^k\}_{k \in \mathbb{N}}$ (Theorem 3.1), we introduce an important Lemma from [23, Lemma 2.5].

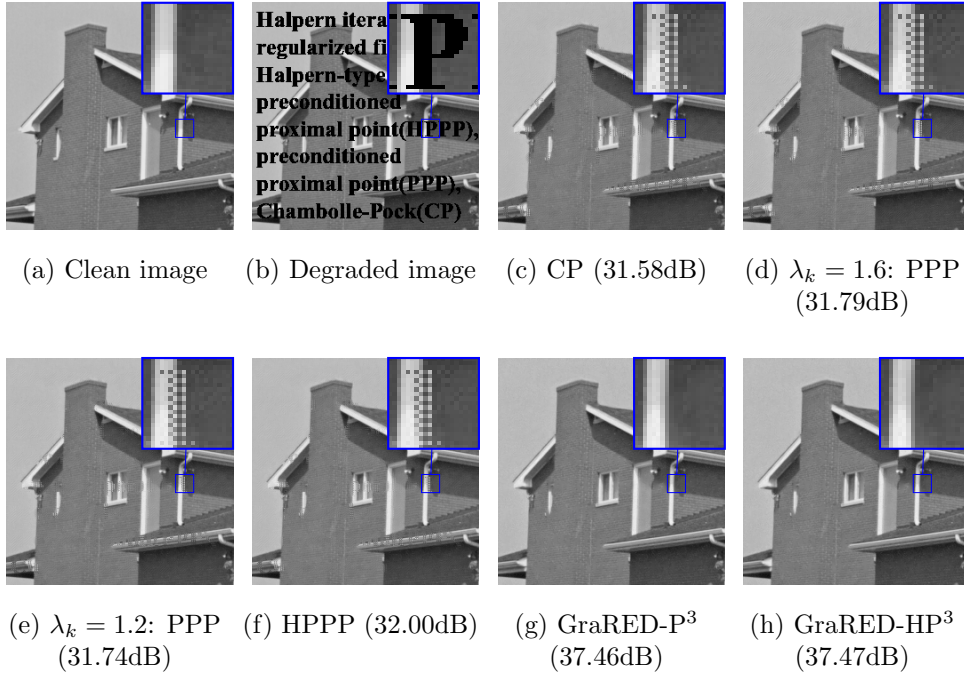


Figure 4.9: Recovery results of **House** degraded by character mask.

Lemma A.1. Let $\{a_k\}_{k \in \mathbb{N}}$ be a sequence of non-negative real numbers satisfying

$$(A.1) \quad a_{k+1} \leq (1 - \mu_k)a_k + \mu_k\beta_k + \gamma_k,$$

where $\{\mu_k\}_{k \in \mathbb{N}}, \{\beta_k\}_{k \in \mathbb{N}}, \{\gamma_k\}_{k \in \mathbb{N}}$ satisfies the following conditions:

- (i) $\{\mu_k\}$ converges to 0 in $[0, 1]$, and $\sum_{k=0}^{\infty} \mu_k = +\infty$, or equivalently $\prod_{k=0}^{\infty} (1 - \mu_k) = 0$;
- (ii) $\limsup_{k \rightarrow \infty} \beta_k \leq 0$;
- (iii) $\gamma_k \geq 0$, $\sum_{k=0}^{\infty} \gamma_k < \infty$.

Then $\lim_{k \rightarrow \infty} a_k = 0$.

Lemma A.2. Let \mathcal{T} be a \mathcal{M} -FNE operator, $(\mathcal{M} + \mathcal{A})^{-1}$ is L -Lipshitz, and $\{\mathbf{u}^k\}$ be the sequence generated by (1.5), $\mathbf{a}, \mathbf{u}^0 \in \mathcal{H}$, and $\lim_{k \rightarrow \infty} \frac{\mu_{k+1} - \mu_k}{\mu_k} = 0$ or $\sum_{k \in \mathbb{N}} |\mu_{k+1} - \mu_k| < \infty$, which satisfies the following:

- (i) $\{\mathbf{u}^k\}, \{\mathcal{T}\mathbf{u}^k\} (k \in \mathbb{N})$ are bounded;
- (ii) $\|\mathcal{T}\mathbf{u}^k - \mathbf{u}^k\|_{\mathcal{M}} \rightarrow 0, k \rightarrow \infty$;
- (iii) $\|\mathbf{u}^{k+1} - \mathbf{u}^k\| \rightarrow 0, \|\mathcal{T}\mathbf{u}^k - \mathbf{u}^k\| \rightarrow 0, k \rightarrow \infty$.

Proof. Let $\mathcal{M} = \mathcal{C}\mathcal{C}^*$ be a decomposition of \mathcal{M} , $C = L\|\mathcal{C}\|$. For $\mathbf{u}', \mathbf{u}'' \in \mathcal{H}$,

$$\begin{aligned} \|\mathcal{T}\mathbf{u}' - \mathcal{T}\mathbf{u}''\| &= \|(\mathcal{M} + \mathcal{A})^{-1}\mathcal{C}\mathcal{C}^*\mathbf{u}' - (\mathcal{M} + \mathcal{A})^{-1}\mathcal{C}\mathcal{C}^*\mathbf{u}''\| \\ &\leq L\|\mathcal{C}\| \|\mathbf{u}' - \mathbf{u}''\|_{\mathcal{M}} = C \|\mathbf{u}' - \mathbf{u}''\|_{\mathcal{M}} \end{aligned}$$

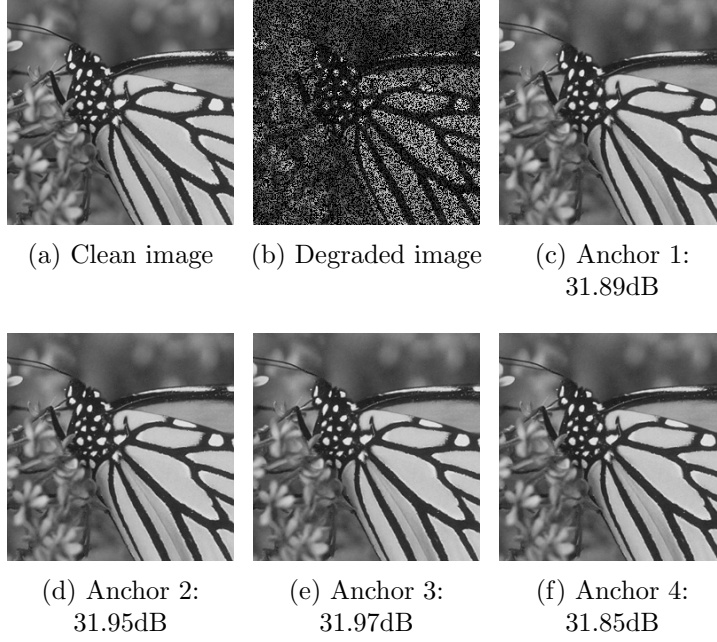


Figure 4.10: Compared with different anchors for random inpainting, i.e., $\mathbf{x}_a = \mathbf{0}, \mathbf{M} \odot \mathbf{x}_0 + 0.5(1 - \mathbf{M}), \mathbf{1}, \mathbf{x}_0$.

For (i), \mathbf{u}^k is bounded. For any $\mathbf{u}^* \in \text{Fix}(T)$,

$$\begin{aligned}
\left\| \mathbf{u}^{k+1} - \mathbf{u}^* \right\|_{\mathcal{M}} &= \left\| \mu_{k+1}(\mathbf{a} - \mathbf{u}^*) + (1 - \mu_{k+1})(\mathcal{T}\mathbf{u}^k - \mathbf{u}^*) \right\|_{\mathcal{M}} \\
&\leq \mu_{k+1} \|\mathbf{a} - \mathbf{u}^*\|_{\mathcal{M}} + (1 - \mu_{k+1}) \left\| \mathbf{u}^k - \mathbf{u}^* \right\|_{\mathcal{M}} \\
&\leq \max\{\|\mathbf{a} - \mathbf{u}^*\|_{\mathcal{M}}, \left\| \mathbf{u}^k - \mathbf{u}^* \right\|_{\mathcal{M}}\} \\
&\leq \dots \leq \max\{\|\mathbf{a} - \mathbf{u}^*\|_{\mathcal{M}}, \left\| \mathbf{u}^0 - \mathbf{u}^* \right\|_{\mathcal{M}}\}.
\end{aligned}$$

Furthermore,

$$\begin{aligned}
\left\| \mathbf{u}^{k+1} - \mathbf{u}^* \right\| &\leq \mu_{k+1} \|\mathbf{a} - \mathbf{u}^*\| + (1 - \mu_{k+1}) \left\| \mathcal{T}\mathbf{u}^k - \mathbf{u}^* \right\| \\
&\leq \mu_{k+1} \|\mathbf{a} - \mathbf{u}^*\| + (1 - \mu_{k+1}) \cdot C \left\| \mathbf{u}^k - \mathbf{u}^* \right\|_{\mathcal{M}} \\
&\leq \max\{\|\mathbf{a} - \mathbf{u}^*\|, C \left\| \mathbf{u}^k - \mathbf{u}^* \right\|_{\mathcal{M}}\} < +\infty.
\end{aligned}$$

and

$$\left\| \mathcal{T}\mathbf{u}^k - \mathbf{u}^* \right\| \leq C \left\| \mathbf{u}^k - \mathbf{u}^* \right\|_{\mathcal{M}} < +\infty$$

So is the sequence $\{\mathcal{T}\mathbf{u}^k\}_{k \in \mathbb{N}}$.

For (ii), we should show \mathcal{T} is \mathcal{M} -asymptotically regular $\|\mathcal{T}\mathbf{u}^k - \mathbf{u}^k\| \rightarrow 0$.
 $\mathbf{u}^{k+1} = \mu_{k+1}\mathbf{a} + (1 - \mu_{k+1})\mathcal{T}\mathbf{u}^k$. There exists a positive real number $M > 0$ such that

$$\|\mathbf{a} - \mathcal{T}\mathbf{u}^k\|_{\mathcal{M}} \leq \|\mathbf{a} - \mathbf{u}^*\|_{\mathcal{M}} + \|\mathbf{u}^k - \mathbf{u}^*\|_{\mathcal{M}} \leq M,$$

it follows from the \mathcal{M} -FNE operator \mathcal{T} and boundedness of $\{\|\mathbf{a} - \mathcal{T}\mathbf{u}^k\|_{\mathcal{M}}\}_{k \in \mathbb{N}}$,

$$\begin{aligned} \|\mathbf{u}^{k+1} - \mathbf{u}^k\|_{\mathcal{M}} &= \|(\mu_{k+1} - \mu_k)(\mathbf{a} - \mathcal{T}\mathbf{u}^{k-1}) + (1 - \mu_{k+1})(\mathcal{T}\mathbf{u}^k - \mathcal{T}\mathbf{u}^{k-1})\|_{\mathcal{M}} \\ (A.2) \quad &\leq (1 - \mu_{k+1})\|\mathcal{T}\mathbf{u}^k - \mathcal{T}\mathbf{u}^{k-1}\|_{\mathcal{M}} + |\mu_{k+1} - \mu_k|\|\mathbf{a} - \mathcal{T}\mathbf{u}^{k-1}\|_{\mathcal{M}} \\ &\leq (1 - \mu_{k+1})\|\mathbf{u}^k - \mathbf{u}^{k-1}\|_{\mathcal{M}} + |\mu_{k+1} - \mu_k| M \end{aligned}$$

If $\lim_{k \rightarrow \infty} \frac{\mu_{k+1} - \mu_k}{\mu_k} = 0$ or $\sum_{k \in \mathbb{N}} |\mu_{k+1} - \mu_k| < \infty$, then $\|\mathbf{u}^{k+1} - \mathbf{u}^k\|_{\mathcal{M}} \rightarrow 0$ from Lemma A.1.

$$\begin{aligned} \|\mathbf{u}^k - \mathcal{T}\mathbf{u}^k\|_{\mathcal{M}} &= \|\mathbf{u}^k - \mathbf{u}^{k+1} + \mathbf{u}^{k+1} - \mathcal{T}\mathbf{u}^k\|_{\mathcal{M}} \\ (A.3) \quad &\leq \|\mathbf{u}^k - \mathbf{u}^{k+1}\|_{\mathcal{M}} + \mu_{k+1}\|\mathbf{a} - \mathcal{T}\mathbf{u}^k\|_{\mathcal{M}}. \end{aligned}$$

Thus, $\lim_{k \rightarrow \infty} \|\mathbf{u}^k - \mathcal{T}\mathbf{u}^k\|_{\mathcal{M}} \rightarrow 0$.

For (iii), there exists M' such that $\|\mathbf{u}^0 - \mathcal{T}\mathbf{u}^{k-1}\| \leq M'$,

$$\begin{aligned} \|\mathbf{u}^{k+1} - \mathbf{u}^k\| &\leq (1 - \mu_{k+1})\|\mathcal{T}\mathbf{u}^k - \mathcal{T}\mathbf{u}^{k-1}\| + |\mu_{k+1} - \mu_k|\|\mathbf{u}^0 - \mathcal{T}\mathbf{u}^{k-1}\| \\ &\leq C(1 - \mu_{k+1})\|\mathbf{u}^k - \mathbf{u}^{k-1}\|_{\mathcal{M}} + M'|\mu_{k+1} - \mu_k|, \end{aligned}$$

Therefore $\|\mathbf{u}^{k+1} - \mathbf{u}^k\| \rightarrow 0$.

$$\|\mathbf{u}^k - \mathcal{T}\mathbf{u}^k\| \leq \|\mathbf{u}^k - \mathbf{u}^{k+1}\| + \mu_{k+1}\|\mathbf{a} - \mathcal{T}\mathbf{u}^k\| \rightarrow 0, k \rightarrow \infty. \quad \blacksquare$$

Lemma A.3. Let $\mathcal{A} : \mathcal{H} \rightarrow 2^{\mathcal{H}}$ be an operator with $\text{zer}\mathcal{A} \neq \emptyset$, and \mathcal{M} an admissible preconditioner such that $\|\mathcal{T}\mathbf{u} - \mathcal{T}\mathbf{v}\| \leq C\|\mathbf{u} - \mathbf{v}\|_{\mathcal{M}}$ ($C > 0$), and $\text{Fix}(\mathcal{T})$ be a closed convex subset of a Hilbert space \mathcal{H} , and $\|\mathbf{u} - \mathbf{a}\|_{\mathcal{M}}^2$ is a proper lower-semicontinuous differentiable convex function. There exists a unique solution $\mathbf{u}^* = \arg \min_{\mathbf{u} \in \text{Fix}(\mathcal{T})} \|\mathbf{u} - \mathbf{a}\|_{\mathcal{M}}^2$ which solves:

$$(A.4) \quad \langle \mathbf{u}^* - \mathbf{a}, \mathbf{u} - \mathbf{u}^* \rangle_{\mathcal{M}} \geq 0, \forall \mathbf{u} \in \text{Fix}(\mathcal{T}).$$

Proof. Let $l(\mathbf{u}) = \|\mathbf{u} - \mathbf{a}\|_{\mathcal{M}}^2$ is the differentiable convex function. Assume that $\mathbf{u}^* \in \text{Fix}(\mathcal{T})$ is the optimal solution, $\text{Fix}(\mathcal{T})$ is the convex set, thus $t \in (0, 1)$, $\mathbf{u}^* + t(\mathbf{u} - \mathbf{u}^*) \in \text{Fix}(\mathcal{T})$ for $\forall \mathbf{u} \in \text{Fix}(\mathcal{T})$,

$$\begin{aligned} \lim_{t \rightarrow 0} \frac{l(\mathbf{u}^* + t(\mathbf{u} - \mathbf{u}^*)) - l(\mathbf{u}^*)}{t} &= \langle l'(\mathbf{u}^*), \mathbf{u} - \mathbf{u}^* \rangle \\ &= \langle 2\mathcal{M}(\mathbf{u}^* - \mathbf{a}), \mathbf{u} - \mathbf{u}^* \rangle \\ &= 2 \langle \mathbf{u}^* - \mathbf{a}, \mathbf{u} - \mathbf{u}^* \rangle_{\mathcal{M}} \geq 0. \end{aligned}$$

If \mathbf{u}^{**} is the another solution such that $\langle \mathbf{u}^{**} - \mathbf{a}, \mathbf{u} - \mathbf{u}^{**} \rangle_{\mathcal{M}} \geq 0$. Replace \mathbf{u} with \mathbf{u}^{**} , \mathbf{u}^* in the above two inequalities, respectively.

$$(A.5) \quad \langle \mathbf{u}^* - \mathbf{a}, \mathbf{u}^{**} - \mathbf{u}^* \rangle_{\mathcal{M}} \geq 0,$$

$$(A.6) \quad \langle \mathbf{u}^{**} - \mathbf{a}, \mathbf{u}^* - \mathbf{u}^{**} \rangle_{\mathcal{M}} \geq 0.$$

If we add two inequalities, then we obtain $\|\mathbf{u}^* - \mathbf{u}^{**}\|_{\mathcal{M}} = 0$. Since

$$\|\mathbf{u}^* - \mathbf{u}^{**}\| = \|\mathcal{T}\mathbf{u}^* - \mathcal{T}\mathbf{u}^{**}\| \leq C \|\mathbf{u}^* - \mathbf{u}^{**}\|_{\mathcal{M}} = 0$$

It follows $\mathbf{u}^* = \mathbf{u}^{**}$ from above inequality. ■

As mentioned in [2, 9] and uniqueness projection onto $\text{Fix}(\mathcal{T})$, we can introduce the following notion of \mathcal{M} -projection.

Definition A.4 (\mathcal{M} -projection). Assume $\forall \mathbf{u}^0 \in \mathcal{H}$, there exist an unique point $\mathbf{u}^* \in \text{Fix}(\mathcal{T})$ such that $\|\mathbf{u}^* - \mathbf{u}^0\|_{\mathcal{M}} \leq \|\mathbf{u} - \mathbf{u}^0\|_{\mathcal{M}}$ ($\forall \mathbf{u} \in \text{Fix}(\mathcal{T})$), then \mathbf{u}^* is called the \mathcal{M} -projection of \mathbf{u}^0 onto $\text{Fix}(\mathcal{T})$, also denoted $P_{\text{Fix}(\mathcal{T})}^{\mathcal{M}}(\mathbf{u}^0)$.

Lemma A.5. Let $\mathcal{T} = (\mathcal{M} + \mathcal{A})^{-1}\mathcal{M}$ such that $\|\mathcal{T}\mathbf{u} - \mathcal{T}\mathbf{v}\| \leq C\|\mathbf{u} - \mathbf{v}\|_{\mathcal{M}}$ ($C > 0$) and $\mathbf{u}^0 \in \mathcal{H}$, then the following conditions are equivalent:

- (i) $\mathbf{u}^* = P_{\text{Fix}(\mathcal{T})}^{\mathcal{M}}(\mathbf{u}^0)$;
- (ii) $\langle \mathbf{u}^* - \mathbf{u}^0, \mathbf{u} - \mathbf{u}^* \rangle_{\mathcal{M}} \geq 0, \forall \mathbf{u} \in \text{Fix}(\mathcal{T})$.

Proof. See Lemma A.3 and Definition A.4. ■

REFERENCES

- [1] H. H. BAUSCHKE AND P. L. COMBETTES, *Convex analysis and monotone operator theory in Hilbert spaces*, CMS Books in Mathematics/Ouvrages de Mathématiques de la SMC, Springer, Cham, second ed., 2017.
- [2] H. H. BAUSCHKE, W. M. MOURSI, S. SINGH, AND X. WANG, *On the bredies-chenchene-lorenz-naldi algorithm*, 2023, <https://arxiv.org/abs/2307.09747>.
- [3] H. H. BAUSCHKE, W. M. MOURSI, AND X. WANG, *Generalized monotone operators and their averaged resolvents*, *Mathematical Programming*, 189 (2021), pp. 55–74, <https://doi.org/10.1007/s10107-020-01500-6>, <https://doi.org/10.1007/s10107-020-01500-6>.
- [4] A. BECK, *First-order methods in optimization*, SIAM, 2017.
- [5] K. BREDIES, E. CHENCHENE, D. A. LORENZ, AND E. NALDI, *Degenerate preconditioned proximal point algorithms*, *SIAM Journal on Optimization*, 32 (2022), pp. 2376–2401, <https://doi.org/10.1137/21M1448112>, <https://doi.org/10.1137/21M1448112>, <https://arxiv.org/abs/https://doi.org/10.1137/21M1448112>.
- [6] K. BREDIES AND H. SUN, *Preconditioned douglas–rachford splitting methods for convex-concave saddle-point problems*, *SIAM Journal on Numerical Analysis*, 53 (2015), pp. 421–444, <https://doi.org/10.1137/140965028>, <https://doi.org/10.1137/140965028>, <https://arxiv.org/abs/https://doi.org/10.1137/140965028>.
- [7] K. BREDIES AND H. SUN, *A proximal point analysis of the preconditioned alternating direction method of multipliers*, *Journal of Optimization Theory and Applications*, 173 (2017), pp. 878–907, <https://doi.org/10.1007/s10957-017-1112-5>, <https://doi.org/10.1007/s10957-017-1112-5>.
- [8] G. T. BUZZARD, S. H. CHAN, S. SREEHARI, AND C. A. BOUMAN, *Plug-and-play unplugged: Optimization-free reconstruction using consensus equilibrium*, *SIAM Journal on Imaging Sciences*, 11 (2018), pp. 2001–2020, <https://doi.org/10.1137/17M1122451>, <https://doi.org/10.1137/17M1122451>, <https://arxiv.org/abs/https://doi.org/10.1137/17M1122451>.

-
- [9] M. N. BÙI AND P. L. COMBETTES, *Warped proximal iterations for monotone inclusions*, Journal of Mathematical Analysis and Applications, 491 (2020), p. 124315, <https://doi.org/10.1016/j.jmaa.2020.124315>, <https://www.sciencedirect.com/science/article/pii/S0022247X20304777>.
- [10] A. CHAMBOLLE AND T. POCK, *A first-order primal-dual algorithm for convex problems with applications to imaging*, Journal of Mathematical Imaging and Vision, 40 (2011), pp. 120–145, <https://doi.org/10.1007/s10851-010-0251-1>.
- [11] S. H. CHAN, X. WANG, AND O. A. ELGENDY, *Plug-and-play admm for image restoration: Fixed-point convergence and applications*, IEEE Transactions on Computational Imaging, 3 (2017), pp. 84–98, <https://doi.org/10.1109/TCI.2016.2629286>.
- [12] Y. CHEN AND T. POCK, *Trainable nonlinear reaction diffusion: A flexible framework for fast and effective image restoration*, IEEE Transactions on Pattern Analysis and Machine Intelligence, 39 (2017), pp. 1256–1272, <https://doi.org/10.1109/TPAMI.2016.2596743>.
- [13] R. COHEN, Y. BLAU, D. FREEDMAN, AND E. RIVLIN, *It has potential: Gradient-driven denoisers for convergent solutions to inverse problems*, in Advances in Neural Information Processing Systems, M. Ranzato, A. Beygelzimer, Y. Dauphin, P. Liang, and J. W. Vaughan, eds., vol. 34, Curran Associates, Inc., 2021, pp. 18152–18164, https://proceedings.neurips.cc/paper_files/paper/2021/file/97108695bd93b6be52fa0334874c8722-Paper.pdf.
- [14] R. COHEN, M. ELAD, AND P. MILANFAR, *Regularization by denoising via fixed-point projection (red-pro)*, SIAM Journal on Imaging Sciences, 14 (2021), pp. 1374–1406.
- [15] J. DIAKONIKOLAS, *Halpern iteration for near-optimal and parameter-free monotone inclusion and strong solutions to variational inequalities*, in Proceedings of Thirty Third Conference on Learning Theory, J. Abernethy and S. Agarwal, eds., vol. 125 of Proceedings of Machine Learning Research, PMLR, 09–12 Jul 2020, pp. 1428–1451, <https://proceedings.mlr.press/v125/diakonikolas20a.html>.
- [16] J. ECKSTEIN AND D. P. BERTSEKAS, *On the douglas—rachford splitting method and the proximal point algorithm for maximal monotone operators*, Mathematical Programming, 55 (1992), pp. 293–318, <https://doi.org/10.1007/BF01581204>.
- [17] H. W. ENGL, M. HANKE, AND A. NEUBAUER, *Regularization of inverse problems*, vol. 375, Springer Science & Business Media, 1996.
- [18] R. GRIBONVAL AND M. NIKOLOVA, *A characterization of proximity operators*, Journal of Mathematical Imaging and Vision, 62 (2020), pp. 773–789, <https://doi.org/10.1007/s10851-020-00951-y>.
- [19] B. HALPERN, *Fixed points of nonexpanding maps*, Bulletin of the American Mathematical Society, 73 (1967), pp. 957–961.
- [20] B. HE AND X. YUAN, *Convergence analysis of primal-dual algorithms for a saddle-point problem: From contraction perspective*, SIAM Journal on Imaging Sciences, 5 (2012), pp. 119–149, <https://doi.org/10.1137/100814494>, <https://arxiv.org/abs/https://doi.org/10.1137/100814494>.
- [21] B. HE AND X. YUAN, *On the convergence rate of douglas—rachford operator splitting method*, Mathematical Programming, 153 (2015), pp. 715–722, <https://doi.org/10.1007/s10107-014-0805-x>.
- [22] S. HE, H.-K. XU, Q.-L. DONG, AND N. MEI, *Convergence analysis of the halpern iteration with adaptive anchoring parameters*, Mathematics of Computation, 93 (2024), pp. 327–345.
- [23] X. U. HONG-KUN, *Iterative algorithms for nonlinear operators*, Journal of the London Mathematical Society, 66 (2002), pp. 240–256.
- [24] S. HURAUULT, A. LECLAIRE, AND N. PAPADAKIS, *Gradient step denoiser for convergent plug-and-play*, ArXiv, abs/2110.03220 (2021), <https://api.semanticscholar.org/CorpusID:238419652>.
- [25] S. HURAUULT, A. LECLAIRE, AND N. PAPADAKIS, *Proximal denoiser for convergent plug-and-play optimization with nonconvex regularization*, in International Conference on Machine Learning, PMLR, 2022, pp. 9483–9505.
- [26] P.-L. LIONS, *Approximation de points fixes de contractions*, CR Acad. Sci. Paris Serie, AB, 284 (1977), pp. 1357–1359.
- [27] G. J. MINTY, *Monotone (nonlinear) operators in hilbert space*, Duke Mathematical Journal, 29 (1962), pp. 341–346, <https://api.semanticscholar.org/CorpusID:121956938>.
- [28] J.-J. MOREAU, *Proximité et dualité dans un espace hilbertien*, Bulletin de la Société mathématique de

- France, 93 (1965), pp. 273–299.
- [29] J. PARK AND E. K. RYU, *Exact optimal accelerated complexity for fixed-point iterations*, in Proceedings of the 39th International Conference on Machine Learning, K. Chaudhuri, S. Jegelka, L. Song, C. Szepesvari, G. Niu, and S. Sabato, eds., vol. 162 of Proceedings of Machine Learning Research, PMLR, 17–23 Jul 2022, pp. 17420–17457, <https://proceedings.mlr.press/v162/park22c.html>.
- [30] T. POCK AND A. CHAMBOLLE, *Diagonal preconditioning for first order primal-dual algorithms in convex optimization*, in 2011 International Conference on Computer Vision, 2011, pp. 1762–1769, <https://doi.org/10.1109/ICCV.2011.6126441>.
- [31] H. QI AND H.-K. XU, *Convergence of halpern’s iteration method with applications in optimization*, Numerical Functional Analysis and Optimization, 42 (2021), pp. 1839–1854, <https://doi.org/10.1080/01630563.2021.2001826>.
- [32] R. T. ROCKAFELLAR, *Monotone operators and the proximal point algorithm*, SIAM Journal on Control and Optimization, 14 (1976), pp. 877–898, <https://doi.org/10.1137/0314056>, <https://doi.org/10.1137/0314056>, <https://arxiv.org/abs/https://doi.org/10.1137/0314056>.
- [33] Y. ROMANO, M. ELAD, AND P. MILANFAR, *The little engine that could: Regularization by denoising (red)*, SIAM Journal on Imaging Sciences, 10 (2017), pp. 1804–1844, <https://doi.org/10.1137/16M1102884>, <https://doi.org/10.1137/16M1102884>, <https://arxiv.org/abs/https://doi.org/10.1137/16M1102884>.
- [34] L. I. RUDIN, S. OSHER, AND E. FATEMI, *Nonlinear total variation based noise removal algorithms*, Physica D: Nonlinear Phenomena, 60 (1992), pp. 259–268, [https://doi.org/https://doi.org/10.1016/0167-2789\(92\)90242-F](https://doi.org/https://doi.org/10.1016/0167-2789(92)90242-F), <https://www.sciencedirect.com/science/article/pii/016727899290242F>.
- [35] E. RYU, J. LIU, S. WANG, X. CHEN, Z. WANG, AND W. YIN, *Plug-and-play methods provably converge with properly trained denoisers*, in International Conference on Machine Learning, PMLR, 2019, pp. 5546–5557.
- [36] S. SABACH AND S. SHTERN, *A first order method for solving convex bilevel optimization problems*, SIAM Journal on Optimization, 27 (2017), pp. 640–660, <https://doi.org/10.1137/16M105592X>, <https://doi.org/10.1137/16M105592X>, <https://arxiv.org/abs/https://doi.org/10.1137/16M105592X>.
- [37] H. Y. TAN, S. MUKHERJEE, J. TANG, AND C.-B. SCHÖNLIEB, *Provably convergent plug-and-play quasi-newton methods*, SIAM Journal on Imaging Sciences, 17 (2024), pp. 785–819, <https://doi.org/10.1137/23M157185X>, <https://doi.org/10.1137/23M157185X>, <https://arxiv.org/abs/https://doi.org/10.1137/23M157185X>.
- [38] S. V. VENKATAKRISHNAN, C. A. BOUMAN, AND B. WOHLBERG, *Plug-and-play priors for model based reconstruction*, in 2013 IEEE Global Conference on Signal and Information Processing, 2013, pp. 945–948, <https://doi.org/10.1109/GlobalSIP.2013.6737048>.
- [39] R. WITTMANN, *Approximation of fixed points of nonexpansive mappings*, Archiv der Mathematik, 58 (1992), pp. 486–491, <https://doi.org/10.1007/BF01190119>, <https://doi.org/10.1007/BF01190119>.
- [40] F. XUE, *A generalized forward-backward splitting operator: degenerate analysis and applications*, Computational and Applied Mathematics, 42 (2022), p. 9, <https://doi.org/10.1007/s40314-022-02143-3>, <https://doi.org/10.1007/s40314-022-02143-3>.
- [41] I. YAMADA, *The hybrid steepest descent method for the variational inequality problem over the intersection of fixed point sets of nonexpansive mappings*, Inherently parallel algorithms in feasibility and optimization and their applications, 8 (2001), pp. 473–504.
- [42] I. YAMADA AND N. OGURA, *Hybrid steepest descent method for variational inequality problem over the fixed point set of certain quasi-nonexpansive mappings*, Numerical Functional Analysis and Optimization, 25 (2005), pp. 619–655, <https://doi.org/10.1081/NFA-200045815>, <https://doi.org/10.1081/NFA-200045815>, <https://arxiv.org/abs/https://doi.org/10.1081/NFA-200045815>.
- [43] K. ZHANG, Y. LI, W. ZUO, L. ZHANG, L. VAN GOOL, AND R. TIMOFTE, *Plug-and-play image restoration with deep denoiser prior*, IEEE Transactions on Pattern Analysis and Machine Intelligence, (2021).
- [44] K. ZHANG, L. VAN GOOL, AND R. TIMOFTE, *Deep unfolding network for image super-resolution*, in 2020 IEEE/CVF Conference on Computer Vision and Pattern Recognition (CVPR), 2020, pp. 3214–3223, <https://doi.org/10.1109/CVPR42600.2020.00328>.
- [45] K. ZHANG, W. ZUO, Y. CHEN, D. MENG, AND L. ZHANG, *Beyond a gaussian denoiser: Residual learning of deep cnn for image denoising*, IEEE Transactions on Image Processing, 26 (2017), pp. 3142–3155, <https://doi.org/10.1109/TIP.2017.2662206>.